[redacted]

PAPER P-743

# LOW-LIGHT-LEVEL PERFORMANCE OF VISUAL SYSTEMS

AD 725831

Alvin D. Schnitzler

March 1971

JUL 6 1971

D

Reproduced by
NATIONAL TECHNICAL
INFORMATION SERVICE
Springfield Va 22151

INSTITUTE FOR DEFENSE ANALYSES
SCIENCE AND TECHNOLOGY DIVISION

IDA Log No. HQ 71-12373
Copy 249 of 350 copies

94

# DISCLAIMER NOTICE

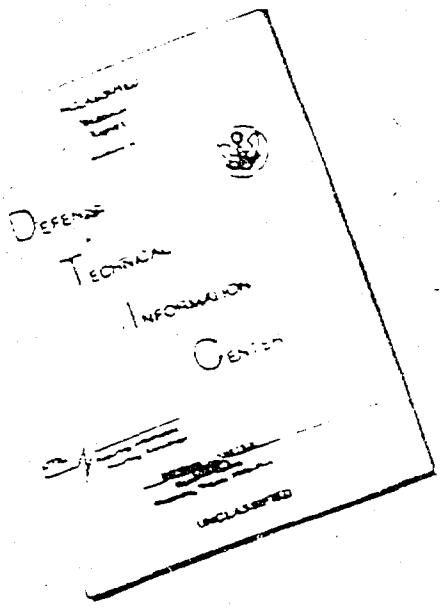


THIS DOCUMENT IS BEST QUALITY AVAILABLE. THE COPY FURNISHED TO DTIC CONTAINED A SIGNIFICANT NUMBER OF PAGES WHICH DO NOT REPRODUCE LEGIBLY.

REPRODUCED FROM
BEST AVAILABLE COPY

ACCESSION for
CFSTI WHITE SECTION
DDC BUFF SECTION
UNANNOUNCED
JUSTIFICATION
BY
DISTRIBUTION/AVAILABILITY CODES
DIST. AVAIL. and/or SPECIAL
A

The work reported in this document was conducted under contract DAHC15 67 C 0011 for the Department of Defense. The publication of this IDA Paper does not indicate endorsement by the Department of Defense, nor should the contents be construed as reflecting the official position of that agency.

Approved for public release; distribution unlimited.

UNCLASSIFIED
Security Classification

**DOCUMENT CONTROL DATA - R & D**

(Security classification of title, body of abstract and indexing annotation must be entered when the overall report is classified)

| | |
|---|---|
| 1. ORIGINATING ACTIVITY (Corporate author)<br>INSTITUTE FOR DEFENSE ANALYSES<br>400 Army-Navy Drive<br>Arlington, Virginia 22202 | 2a. REPORT SECURITY CLASSIFICATION<br>UNCLASSIFIED<br>2b. GROUP<br>-- |

3. REPORT TITLE
Low-Light-Level Performance of Visual Systems

4. DESCRIPTIVE NOTES (Type of report and inclusive dates)
Paper P-743, March 1971

5. AUTHOR(S) (First name, middle initial, last name)
Alvin D. Schnitzler

| | | |
|---|---|---|
| 6. REPORT DATE<br>March 1971 | 7a. TOTAL NO. OF PAGES<br>88 | 7b. NO. OF REFS<br>24 |
| 8a. CONTRACT OR GRANT NO.<br>DAHC15 67 C 0011<br>b. PROJECT NO.<br>Task T-36 | 9a. ORIGINATOR'S REPORT NUMBER(S)<br>P-743<br>9b. OTHER REPORT NO(S) (Any other numbers that may be assigned this report)<br>None | |

10. DISTRIBUTION STATEMENT
Approved for public release; Distribution unlimited

| | |
|---|---|
| 11. SUPPLEMENTARY NOTES<br>NA | 12. SPONSORING MILITARY ACTIVITY<br>Advanced Research Projects Agency<br>Arlington, Virginia 22209 |

13. ABSTRACT

Visual systems for employment at low light levels are examined from two points of view:

1. As extensions of the human visual system and
2. As optical information acquisition and conversion systems.

The first point of view is adopted to examine the general suitability and the limitations of reliance on the dark-adapted human eye alone, the dark-adapted human eye aided by binoculars, and the light-adapted human eye aided by photoelectronic imaging systems such as image intensifiers and low-light-level television. The second point of view is adopted to analyze the dependence of photoelectronic imaging system performance on system parameters. Finally, both points of view are combined to examine the transfer of image information from the display of a photoelectronic imaging system to the output of the eye.

DD FORM 1 NOV 65 1473

UNCLASSIFIED
Security Classification

UNCLASSIFIED
Security Classification

| 14 KEY WORDS | LINK A ROLE | LINK A WT | LINK B ROLE | LINK B WT | LINK C ROLE | LINK C WT |
|---|---|---|---|---|---|---|
| low-light-level television | | | | | | |
| image intensifiers | | | | | | |
| visual systems | | | | | | |

UNCLASSIFIED
Security Classification

PAPER P-743

# LOW-LIGHT-LEVEL PERFORMANCE OF VISUAL SYSTEMS

Alvin D. Schnitzler

March 1971

DISTRIBUTION STATEMENT A
Approved for public release;
Distribution Unlimited

INSTITUTE FOR DEFENSE ANALYSES
SCIENCE AND TECHNOLOGY DIVISION
400 Army-Navy Drive, Arlington, Virginia 22202

Contract DAHC15 67 C 0011
Task T-36

## PREFACE

Exploitation of electrooptical technology has culminated in the successful deployment of night vision systems in the field. The choice of the most direct and efficient means of further improving the performance of night vision systems depends on a thorough understanding of the effect on performance of independent variations of system parameters and of the interactions between them. It is the purpose of this paper to provide the necessary understanding for those who are interested in a full mathematical treatment. A companion IDA report contains a nonmathematical condensation of this paper as well as a review of specific night vision devices. That report is Low-Light-Level Devices: A Components Manual for Systems Designers, IDA Report R-169, by Lucien M. Biberman, Alvin D. Schnitzler, Frederick A. Rosell, Harry L. Snyder, and Otto H. Schade, Sr.

This paper is one in a series under ODDR&E Task T-36, Infrared and Night Vision. The program is responsive to E. N. Myers, Electronics Information Systems, ODDR&E.

## SYMBOLS

| | |
|---|---|
| $A$ | area of aperture |
| $A_o$ | area of entrance pupil |
| $A_s$ | area of image formed by visual system on retina |
| $A_u$ | area of image formed by unaided eye on retina |
| $B$ | luminance |
| $e$ | magnitude of electric charge, coulombs |
| $F$ | luminous flux |
| $F_s$ | luminous flux collected by visual system |
| $F_u$ | luminous flux collected by unaided eye |
| $f_O$ | focal length of objective |
| $f_p$ | focal length of eyepiece |
| $G$ | number of photons emitted by display per photoelectron emitted by primary photocathode |
| $G_I$ | electric current gain |
| $H$ | irradiance |
| $H_\lambda$ | spectral irradiance |
| $H_s$ | irradiance at photocathode |
| $h_D$ | height of display |
| $h_T$ | height of target |
| $i$ | electric current |
| $i_s$ | primary photoelectric current |
| $j_D$ | electric current density incident on display |
| $j_S$ | electric current density at photocathode |
| $K_D$ | luminous efficacy of display radiance |
| $K_S$ | luminous efficacy of input irradiance |
| $k_{\lambda D}$ | spectral radiant conversion factor of phosphor |
| $k_{HB}$ | luminous conversion efficiency |
| $L'$ | apparent radiance |

| | |
|---|---|
| $L_D$ | effective length of sine-wave pattern |
| $M_D$ | modulation amplitude on display |
| $M_S$ | modulation amplitude on photocathode |
| $\mathfrak{m}$ | subjective magnification |
| $m$ | magnification |
| $m_I$ | magnification of image intensifier |
| $m_O$ | magnification of eyepiece |
| $m_{PE}$ | magnification of eyepiece-eye subsystem |
| $N$ | number of television lines per raster height |
| $n$ | index of refraction of object space |
| $n'$ | index of refraction of eye |
| $n_s$ | photoelectron flux density |
| $P_\lambda$ | spectral radiant power |
| $R(\lambda)$ | relative spectral response |
| $S$ | separation between display and observer |
| $T(\nu)$ | sine-wave response, frequency response, modulation transfer function |
| $t$ | effective integration time of eye |
| $W_D$ | width of sine-wave half period |
| $Z(\lambda)$ | relative spectral radiant conversion factor |
| $\beta$ | half angle of field of view |
| $\epsilon$ | effective length-to-width ratio of half period of test frequency |
| $\bar{\eta}$ | mean quantum efficiency |
| $\eta_c$ | collection efficiency |
| $\eta_E$ | quantum efficiency of eye |
| $\theta_E$ | angle subtended by eye radius at object |
| $\theta_O$ | angle subtended by entrance pupil radius at object |
| $\theta'_O$ | angle subtended by exit pupil radius at image |
| $\theta_{PE}$ | angle subtended by eyepiece-eye entrance pupil radius at display |
| $\lambda$ | wavelength of radiation |
| $\nu$ | sine-wave spatial frequency |
| $\nu_D$ | spatial frequency on display |
| $\nu_R$ | spatial frequency on retina |

| | |
|---|---|
| $\nu_S$ | spatial frequency on photocathode |
| $\rho_c$ | radius of photocathode |
| $\rho_E$ | radius of entrance pupil of eye |
| $\rho_O'$ | radius of exit pupil of objective |
| $\rho_s$ | radius of entrance pupil of visual system |
| $\sigma(\lambda)$ | responsivity of photocathode, amperes per watt |
| $\Omega$ | solid angle |

The most significant findings of the analysis of the performance of photoelectronic imaging systems are the surprisingly weak effect, at a useful light level, of variation in either photocathode responsivity or overall system integration time and the strong effect of variation in the modulation transfer function. The reverse occurs at sufficiently low light levels, but then performance is severely degraded by lack of sufficient signal-to-noise ratio. These results are important to the design and the choice of means for further improvement of image-intensifier and low-light-level television systems.

CONTENTS


I. Introduction 1

II. Low-Light-Level Performance of the Eye 5

III. Low-Light-Level Performance of Binoculars 15

IV. Photoelectronic Imaging Systems 21

A. Optical Parameters and Principle of Operation 21
B. Spectral Response of Photocathodes 28
C. Luminous Conversion Factor of Phosphors 33
D. Temporal Response 39
E. Spatial Frequency Response, Modulation Transfer Function 40

V. Analysis of Photoelectronic Imaging Systems 51

A. Noise-Equivalent Modulation 53
B. Improvement of PEI Performance 63

VI. Conclusions 73

References 75

Appendix A--Image Information Transfer, Display to Eye 77

Appendix B--Required Modulation, Signal-to-Noise Ratio, and Resolution 83

# I. INTRODUCTION

Visual systems designed for operation at low light levels generally fall into two categories, passive optical systems and active photoelectronic systems. The former are represented by night vision binoculars and the latter by image-intensifier and low-light-level television systems.

The utilization of photoelectronic imaging systems at low light levels involves a number of engineering factors:

- The reflection and/or emission of radiant flux by targets and backgrounds.
- The absorption and scattering of radiant flux by the intervening atmosphere.
- The efficiency of collection of radiant flux.
- The efficiency of conversion of radiant flux into luminous flux by the photoelectronic imaging system.

All of these factors could apply to a radiometer as well as to an imaging system. But the purpose of a photoelectronic imaging system is not merely to collect and convert radiant flux into luminous flux.

The purpose of a photoelectronic imaging system is to increase the acquisition and flow of optical information from a scene to an image interpreter over what would be possible if the interpreter were forced to rely on his eyes alone. Hence, a photoelectronic imaging system is part of a communication system. The information source is the scene, the optical information being in the form of a spatial modulation of the radiance of the scene. The transmitter or power source is either the irradiance of the scene by moonlight, starlight, and

airglow or the thermal self-radiance of the scene The transmissive medium is the atmosphere. The communication receiver is the night vision system itself. The user is the image interpreter.

A widespread notion has persisted among many optical engineers that the performance of a photoelectronic imaging system cannot be specified independently of the physical conditions of the scene and the atmosphere as well as the physiological and psychological state of the image interpreter. In communication engineering this would correspond to the notion that a communication receiver cannot be sensibly specified because the output depends on the power and distance of the transmitter, the conditions of the atmosphere, and the state of the operator. But we can and do specify the performance of a communication receiver, essentially by the temporal frequency response or the transfer characteristic and the sensitivity or noise equivalent power. Likewise, the performance of a night vision system may be essentially specified by the spatial frequency response, or the modulation transfer function as it is called in optics, and the noise equivalent modulation.

The performance of a photoelectronic imaging system depends on the fidelity of the conversion of radiant input signals into luminous output signals which appear on the display. This conversion process is degraded by:

- The responsivity of the photocathode,
- The roll-off of the modulation transfer function at the higher spatial frequencies, and by
- The generation of noise in the system.

All three combine to reduce the ratio of signal to noise in the output luminous image and, therefore, the probability of target detection by the image interpreter, where the signal in luminous images is due to the spatial variation of the mean luminance and the noise is due to temporal fluctuations of the luminance. In principle, to the approximation that a photoelectronic imaging system is linear, temporally invariant, and spatially invariant, the luminous output signal and the

radiant input signal can be related by employing the modulation transfer function of the system in the appropriate Fourier transformations. Similarly, the luminous output noise can be related to both the radiant input noise and the electrical system noise by the Wiener transformation. Then the signal-to-noise ratio can be calculated, and the probability of target detection can be estimated.

In practice, except for simple targets such as points, squares, and rectangles, the detailed signal-to-noise ratio analysis of a complex target is too difficult to perform rigorously. However, the output signal-to-noise ratio as a function of the spatial frequency of a one-dimensional sine-wave input signal can be calculated and the resolution frequency--that is, the maximum spatial frequency for which the output signal-to-noise ratio is greater than approximately unity--can be determined. Moreover, it has been shown experimentally that the detection, recognition, and identification probabilities of complex targets are proportional to the number of periods of the resolution frequency subtended by the minimum target dimension presented to the viewer on the display. More periods are required for high probability than for low, for identification than for recognition, and for recognition than for detection. Therefore, if the probabilities are known as a function of resolution frequency and if a signal-to-noise ratio calculation of the resolution frequency of a photoelectronic imaging system is made, then the probabilities for complex targets as a function of minimum dimension and range can be predicted by analysis.

The dependence of the probabilities on the number of periods of the resolution frequency is plausible analytically because the resolution frequency defines the useful spatial bandwidth of the system, i.e., the range of spatial frequencies for which the signal-to-noise ratio is greater than unity. At the same time, the spectral density corresponding to the minimum dimension W of a target is just the sinc function of $\pi\nu W$, where $\nu$ is the spatial frequency. The sinc function is unity at $\nu = 0$, decreases to zero at $\nu = 1/W$, and then undergoes damped oscillations about the frequency axis with increasing frequency. Thus, the spectral density is essentially contained in the

frequency range from 0 to 1/W. If W subtends one period of the resolution frequency, then 1/W is also the resolution frequency. Hence, the useful bandwidth of the system essentially contains the spectral density corresponding to the minimum dimension of the target. Recognition depends on perception of target detail, and hence for a given range and target size more periods of the resolution frequency or greater spatial bandwidths are required.

## II. LOW-LIGHT-LEVEL PERFORMANCE OF THE EYE

A full appreciation of the principles of operation of photoelectronic imaging (PEI) systems depends on knowledge of certain features of the visual process. For this purpose it is useful to examine and compare the operation of visual systems such as the unaided eye and binoculars on the one hand with PEI systems on the other. However, in any comparison of visual systems, in which the retina of the eye is the primary radiation sensor, with physical devices, in which some other radiation-sensitive layer is the primary sensor, one is confronted with the relation between the subjective and objective effects of radiation in the visible and adjacent regions of the spectrum. This relation is particularly important in examining the operation of visual systems incorporating PEI systems, since their overall performance depends on both the physical properties of the input radiation and the subjective properties of the output radiation.

The problem arises because the eye, as shown in Fig. 1, is so selective in its spectral response that radiant power expressed in watts is an inadequate measure of the subjective effect of a flux of radiant energy. Two alternative procedures are available:

1. a. Specify the spectral response of the eye,
   b. Specify the spectral content of the flux, and
   c. Perform a numerical integration of their product over all wavelengths within the passband of the eye.

2. Define an arbitrary unit of luminous flux, spectrally normalized to the peak of human visual response, as an overall measure of the subjective effect of the flux of radiant energy without explicit concern for its spectral content and the spectral response of the eye.

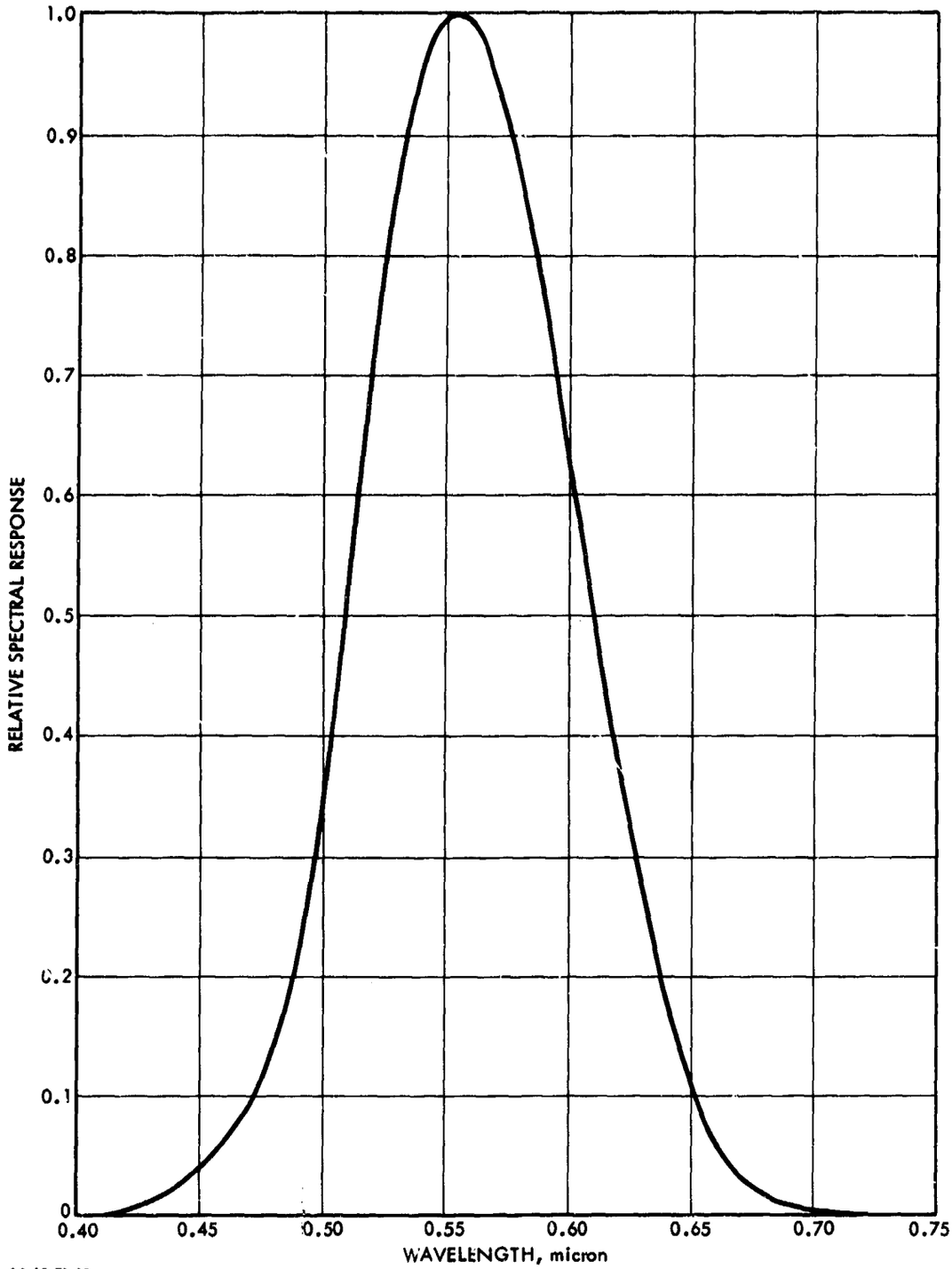


S3-15-71-10

FIGURE 1. Standard Visibility Curve of the Photopic Eye

The second procedure requires the establishment of a standard of luminous flux as a reference to determine the value of unknown luminous flux by comparison. In practice, it is easier to maintain a standard of luminous intensity rather than a standard of luminous flux. The standard of luminous intensity, the candela, is defined as one-sixtieth of the luminous intensity per square centimeter of a blackbody radiator at the temperature of solidification of platinum (approximately $2042^{\circ}K$). The unit of luminous flux, the lumen, is the amount of luminous flux emitted within a unit solid angle by an isotropic point source of luminous intensity equal to one candela. For an extended source of luminous flux, the luminance of an element of surface is defined as the luminous flux that leaves the surface per unit solid angle and unit projected area of the element of surface. If the surface is a perfectly diffuse radiating (or reflecting) surface, the total luminous flux leaving the surface per unit area is equal to $\pi$ times the luminance. The amount of luminous flux incident per unit area of a surface is the illumination of the surface. The unit of illumination, lumen per unit area, depends on the unit of area chosen.

Since the procedure of establishing a unit of luminous flux as an overall measure of the subjective effect of a flux of radiant energy is implicitly dependent on the spectral response of the Commission Internationale de l'Eclairage (CIE) "standard observer," this procedure does not apply to radiation sensors with other spectral responsivities. For general application to all radiation sensors, the first procedure, explicitly taking into account the spectral response of the radiation sensor (e.g., the eye), is superior, for then the radiant power can be expressed in watts without loss of rigor. In the case of the eye, for any spectral distribution of radiant power, one has

$$F = 680 \int_0^{\infty} y(\lambda) P_{\lambda} d\lambda \qquad (1)$$

where F (in lumens) may be viewed either as a luminous flux (i.e., the visual content of the flux of radiant energy) or as a measure of the amount of visual sensation evoked by the radiant power, $y(\lambda)$ is the relative spectral response (better known as the "standard observer" function) of the eye, and $P_\lambda$ is the spectral radiant power in watt/nm. The numerical factor 680 is the luminous equivalent of one watt of radiant power at the peak of the visibility curve [$y(\lambda) = 1$], which for photopic vision occurs at 555 nm.

If a photoelectronic sensor is employed, rather than visual sensation, the output is a directly measurable electric current. In this case, one has

$$i = \sigma(\lambda_p) \int_0^\infty R(\lambda) P_\lambda d\lambda \qquad (2)$$

where i is the electric current in amperes, $\sigma(\lambda_p)$ is the absolute radiant responsivity of the sensor at the peak wavelength in amperes/watt, $R(\lambda)$ is the relative spectral response of the sensor, and $P_\lambda$ is again the spectral radiant power. The evaluation of photocathodes is discussed in detail in Section IV-B.

The physical quantities corresponding to luminance and illuminance are radiance and irradiance. They are based on radiant power in watts. The unit of radiance, depending on the choice of unit of area, is watt per unit area per unit solid angle. Likewise, the unit of irradiance is watt per unit area. A table of some of the corresponding subjective (photometric) and physical (radiometric) quantities is given below:

| Photometric | | Radiometric | |
|---|---|---|---|
| Quantity | Unit | Quantity | Unit |
| Luminous flux | lumen | Radiant flux | watt |
| Luminous intensity | candela* | Radiant intensity | watt/steradian |
| Luminance | candela/ $meter^2$ | Radiance | watt/$meter^2$-steradian |
| Illuminance | lumen/ $meter^2$ | Irradiance | watt/$meter^2$ |

For a more extensive treatment of photometric and radiometric quantities, see, for example, Refs. 1 and 2, among other sources.

In the text below, wherever it is appropriate to take explicit note of the spectral response of the eye or wherever photoelectronic sensors are under consideration, the quantities used will be radiometric.

At low light levels, to compensate for the loss of visual stimuli, the eye automatically undergoes various adjustments. These adjustments include:

- Increasing photon collection by dilation of the pupil.
- Integrating the signal over larger areas on the retina by extracting the signal from larger clusters of elemental sensors.
- Increasing the sensitivity of the retina by means of dark adaptation, which includes switching from less sensitive to more sensitive sensors as well as lowering the sensitivity thresholds of both.
- Integrating the signal over a longer time.

*The candela is defined to yield one lumen per steradian. Thus the unit solid angle is implicit in the definition.

The area of the pupil of the eye is controlled by the iris, a ring-shaped involuntary muscle adjacent to the anterior surface of the lens. It has been shown (Ref. 3) that the pupil area increases by approximately a factor of 10 as the light level decreases from bright sunlight at $10^3$ cd/m$^2$ to the darkness of an overcast night at $10^{-5}$ cd/m$^2$.

The amount of light collected by a circular aperture such as the entrance pupil of the eye is given by

$$F = AB\,\Omega \tag{3}$$

where A is the area of the aperture, B is the luminance of a paraxial object, and $\Omega$ is the solid angle subtended by the object at the aperture. Since an increase in the area of the entrance pupil has no effect on the magnification of the eye, the area of the image on the retina remains unchanged. Hence, by dilation of the pupil retinal illumination increases, image brightness increases, and visual perception at low light levels is improved.

The ability of the eye to integrate the signal over increasing areas of the retina with decreasing light level is shown (Ref. 4) in Fig. 2. The threshold luminance $B_t$ required for perception of an object subtending an angle $\alpha$ at the entrance pupil of the eye decreases with increasing $\alpha^2$, which is proportional to the area of the image on the retina. Data such as are shown in Fig. 2 differ little, whether a disk or a Landolt C-ring is projected on a screen, and for a given $\alpha$ the luminance is increased until the viewer perceives the location of either the disk or the gap in the C-ring. The two portions of the curve in Fig. 2 are due to the presence of two types of sensors: (1) the rods, which respond at low light levels, and (2) the cones, for daylight and color vision.

According to Eq. 3, the luminous flux collected from an object by the eye is proportional to the product of $B_t$ and $\alpha^2$ (since $\Omega \propto \alpha^2$). However, Fig. 2 shows that at low light levels, where vision depends on the rod sensors, the eye becomes quite ineffective at integrating the

signal from elements separated from the center of the object by distances which subtend angles larger than 4 or 5 deg. Thus, as $\alpha$ approaches 4 or 5 deg, the threshold flux increases rapidly. This limitation is shown in Section III to be of special significance for the application of large-aperture binoculars or night glasses to increase visual perception at low light levels.

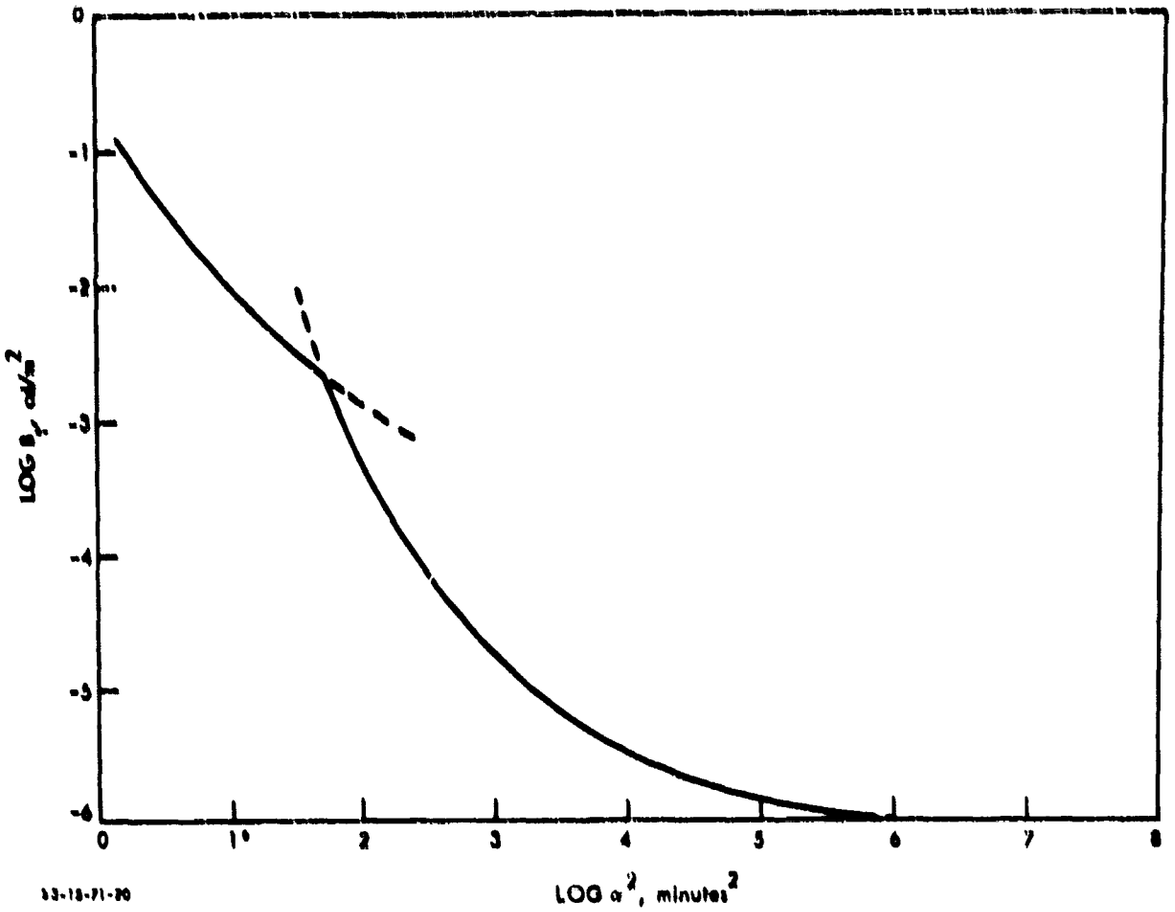


FIGURE 2. Threshold Luminance as a Function of Angle Subtended at Eye Pupil by Disk or Gap in Landolt C-Ring (Ref. 4)

The increase in sensitivity (reduction in visual threshold) that occurs with increasing dark adaptation is illustrated in Fig. 3 (Ref. 5), where the logarithm of threshold luminance versus time of dark adaptation is plotted. The experiments were conducted by preadaptation with approximately 5000 cd/m$^2$ of white light and then determination of the threshold luminance required by the observer to resolve the lines of

a grating. In these experiments, vision is dominated by the cone sensors during the first 7 or 8 min of dark adaptation before the visual threshold of the rod sensors, decreasing more rapidly, becomes dominant. The effect of area on visual threshold, as discussed above, is also evident in Fig. 3. It is interesting to note that the rod sensors cannot resolve lines subtending an angle of 4 min, while the cone sensors can resolve objects of less than 1 min.

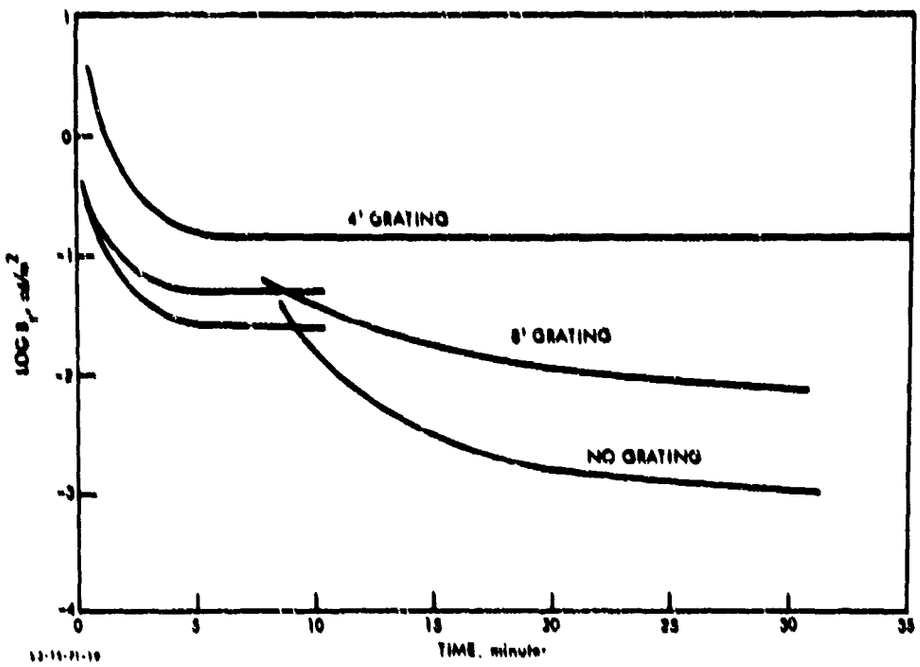


FIGURE 3. Threshold Luminance as a Function of Time During Dark Adaptation Following Preadaptation to 5000 cd/m$^2$ (Ref. 5)

The relatively slow progress of dark adaptation shown in Fig. 3 poses a severe problem for sensitive vision at night if an observer is required to pass from a brightly illuminated artificial environment into a dimly illuminated natural environment or if dark adaptation is destroyed by flashes or occasional sources of light in an otherwise dark scene. For example, under the conditions applying to Fig. 3, if the object luminance were $10^{-2}$ cd/m$^2$, the observer would

have to wait nearly 11 min to become sufficiently dark-adapted to perceive a gross unlined object, and approximately 22 min to resolve a line grating in which a line subtends an angle of 8 min at the eye. Image-intensifier and television systems can be of great value under such conditions, since it is unnecessary to wait for dark adaptation if the output image is presented at sufficient brightness.

The ability of the eye to integrate the signal over a longer time at low light levels appears to be the least important of the response parameter adjustments made to compensate for the decreased photon flux. Rose (Ref. 6), for example, claims that the effective storage or integration time of the eye is close to 0.2 sec and that it varies little from extremely low to high light levels. Schade (Ref. 7), on the other hand, claims that the effective storage time decreases from approximately 0.2 sec at the threshold of vision towards a plateau of approximately 0.05 sec at high illumination.

## III. LOW-LIGHT-LEVEL PERFORMANCE OF BINOCULARS

Limited aid to visual performance at low light levels can be provided by means of purely geometric optic devices such as binoculars. Special care is taken in the design and construction of such devices to ensure maximum transfer of radiation collected by the objective to the retina of the eye. It is essential that the exit pupil of the device is large enough to match the large entrance pupil of the dark-adapted eye. In this case, binoculars will produce the subjective impression of increased image brightness and permit the detection of targets not visible to the unaided eye. This increase in visual performance, the well-known night-glass effect, is shown below to result from the increased size of the image on the retina provided by the subjective magnification of the binoculars. It does not result from more irradiance in the image. Indeed, an increase in image radiance by purely geometric optics would violate the second law of thermodynamics.

The other parameters upon which the detection of a target image depends, such as wavelength, exposure time, contrast, and requirement for dark adaptation, are little affected by night-vision binoculars. The aid to visual performance provided by night-vision binoculars depends solely on the spatial integration capability of the dark-adapted eye, which was described in Section II as relatively ineffective for images viewed in the eyepiece subtending more than 4 to 5 deg at the entrance pupil of the eye.

In any well-designed visual instrument, such as night-vision binoculars, the eye is placed so that the entrance pupil of the eye nearly coincides in position with the exit pupil of the instrument, since placing the eye elsewhere merely introduces an additional stop

that may unnecessarily reduce the field of view. A diagram of the complete visual system is shown in Fig. 4. A detailed discussion of the limitation of rays by apertures will be found in Chapter V of Ref. 3.

By making use of Abbe's sine condition (Ref. 3) and the definition of the subjective magnification $\mathfrak{m}$ as the ratio of the magnification with binoculars to the magnification of the unaided eye, it can be shown that $\mathfrak{m}$ is given by

$$\mathfrak{m} = (\rho_s/\rho_E(\sin \theta_E'/\sin \theta_s') \tag{4}$$

where $\rho_s$ and $\rho_E$ are the radii of the entrance pupils of the visual system and eye, respectively; $\theta_s'$ and $\theta_E'$ are the angles subtended at the image by the radii of exit pupils.

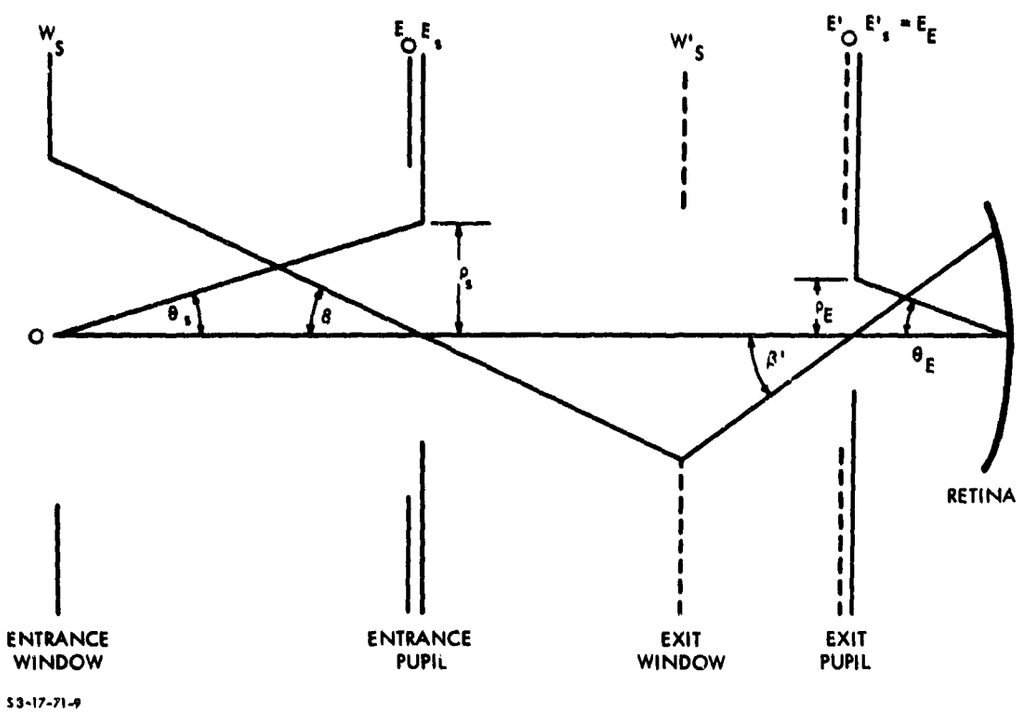


FIGURE 4. Schematic Diagram of Binocular Visual System

According to Eq. 3, the total flux collected from a small object near the optical axis is proportional to the area of the entrance pupil of an optical system. Hence, the relative increase of flux with binoculars compared to the unaided eye is given by

$$F_s/F_u = \rho_s^2/\rho_E^2 \tag{5}$$

where $F_s$ and $F_u$ are the total fluxes collected from an object by the complete visual system and the unaided eye, respectively. Since the illumination in an image is equal to the light flux per unit area, the ratio of the retinal illumination in the images of an object produced by the complete visual system and the unaided eye, respectively, is given by

$$E_s/E_u = (F_s/A_s)/(F_u/A_u) \tag{6}$$

where $A_s$ and $A_u$ are the image areas for the complete visual system and the unaided eye, respectively. By combining Eqs. 4 to 6, one obtains

$$E_s/E_u = \sin^2 \theta_s'/\sin^2 \theta_E'. \tag{7}$$

By referring to Fig. 4, it is clear that, if $\theta_E' \leq \theta_O'$, then the eye pupil is the aperture stop of the complete system, $\theta_s' = \theta_E'$, and

$$E_s/E_u = 1. \tag{8}$$

On the other hand, if $\theta_E' > \theta_O'$, the aperture stop of the binoculars is the aperture stop of the system, $\theta_s' = \theta_O'$, and

$$E_s/E_u = \sin^2 \theta_O'/\sin^2 \theta_E' \tag{9}$$

i.e., $E_s/E_u$ is less than unity. Thus, one sees that binoculars cannot provide an increase in retinal image illumination, and increasing visual perception with such instruments will depend on the effect described below.

Clearly, good design requires that the eye pupil be the aperture stop of the system so that, except for whatever reduction results from transmission losses in the lenses, retinal image illumination will be as great with binoculars as with the unaided eye. Then $\theta_E' = \theta_s'$, and by Eq. 4 the subjective magnification is simply

$$\mathfrak{m} = \rho_s/\rho_E \tag{10}$$

and by Eq. 5

$$F_s/F_u = \mathfrak{m}^2. \tag{11}$$

Equations 10 and 11 show that use of binoculars results in the formation of a larger image on the retina (in proportion to $\mathfrak{m}^2$), which, neglecting transmission losses, exactly balances an increase in photon collection efficiency. Thus, the increase in visual perception provided by binoculars depends on the spatial integration capability of the eye, illustrated in Fig. 2, to lower the luminance threshold. For nearby objects too small to be resolved at a given light level, subjective magnification may increase the image area on the retina sufficiently for visual perception. Such an effect is limited, however, by the limited ability of the eye to summate the signals from a large number of elemental sensors.

To produce a sharply defined field of view in a visual instrument, the field stop is usually placed so that its image (the entrance window) in object space lies in the object plane and its image (the exit window) in image space is in the image plane. Then, by the definition of $\mathfrak{m}$, the angle $\beta'$, subtended at the exit pupil by the radius of the exit window, is related to the angle $\beta$, subtended at the entrance pupil by the radius of the entrance window, by the equation

$$\beta' = m\beta. \tag{12}$$

The angle $\beta'$ of a well-corrected eyepiece is limited to approximately 0.5 radian (i.e., the full angular field of view of an eyepiece is limited to approximately 1.0 radian), and consequently, for even small values of the subjective magnification, $\beta$ is severely restricted.

The increase in visual perception at low light levels realized with binoculars may be attributed to the increase in image area on the retina produced by the subjective magnification and depends on the limited ability of the eye to integrate the signal over the increased image area. High subjective magnification is required for target detection, but the field of view, which is of major importance in visual search operations, is reduced in proportion to the increase in retinal image area. Thus, binoculars increase the probability of detection if the object is within the field of view but decrease the probability that the visual field includes the object to be detected.

## IV. PHOTOELECTRONIC IMAGING SYSTEMS

### A. OPTICAL PARAMETERS AND PRINCIPLE OF OPERATION

The incorporation of PEI devices in visual systems permits the manipulation of design parameters with far greater flexibility than allowed with binoculars. Image-intensifier night-vision systems incorporate an objective for collecting and focusing the radiant flux emanating from the scene onto the fiber-optic faceplate of an image-intensifier tube, an image-intensifier tube usually containing three stages of intensification, and an eyepiece presenting an enlarged virtual image of the intensifier display. Low-light-level television systems incorporate the following: an objective, one or more intensifier modules, a camera tube, fiber-optic couplers, a video signal amplifier, and a monitor containing a kinescope for displaying a real image for viewing. The incorporation of PEI devices in visual systems has the effect of decoupling the input and output radiant fluxes, removing some of the optical constraints encountered in binocular systems, such as those on:

- The utilization of radiant flux outside the visible spectrum and generally the use of more efficient image sensors than the eye.
- Independent adjustments of subjective magnification and flux collection power.
- The use of integration times longer than that of the eye.
- The time required for dark adaptation (dark adaptation is not required).
- The independent choice of optimum image brightness for high visual acuity and freedom from eyestrain.

**Preceding page blank**

In addition, PEI systems may provide greater flexibility of viewing through the use of remote-view television techniques. In practice, limitations on the performance of PEI systems arise because of imperfect technology and practical restrictions on size, weight, and cost.

1. Image-Intensifier Systems

In visual systems incorporating image intensifiers, the three parameters, (1) subjective magnification, (2) collection power, and (3) field of view, can be adjusted independently, in contrast to binocular visual systems. In addition, the threshold sensitivity, quantum efficiency, and integration time of the system are subject to optimization to increase visual perception at low values of scene radiance. Each of the parameters will be considered in turn, beginning with subjective magnification.

A diagram of a complete image-intensifier visual system, comprising an optical objective, an image intensifier, an eyepiece, and the eye, is shown in Fig. 5. The magnification $m_s$ between the retinal image and a distant object viewed through an image-intensifier system is given by

$$m_s = m_O \, m_I \, m_{PE} \tag{13}$$

where $m_O$ is the magnification of the objective, $m_I$ is the magnification of the image intensifier, and $m_{PE}$ is the magnification of the subsystem, consisting of the eyepiece and the eye together. By Abbe's sine condition, $m_O$ is given by

$$m_O = \sin \theta_O / \sin \theta_O' \tag{14}$$

where $\theta_O$ is the angle subtended by the radius of the entrance pupil at the object and $\theta_O'$ is the angle subtended by the radius of the exit pupil at the image that falls on the sensor surface of the image intensifier. The magnification of the eyepiece and eye subsystem is given by

$$m_{PE} = (n/n')(\sin \theta_{PE}/\sin \theta'_{PE}) \qquad (15)$$

where n and n′ are the indices of refraction of the object space and the eye, respectively, $\theta_{PE}$ is the angle subtended by the radius of the entrance pupil of the subsystem at the display surface of the image intensifier, and $\theta'_{PE}$ is the angle subtended by the radius of the exit pupil of the subsystem at the retina.

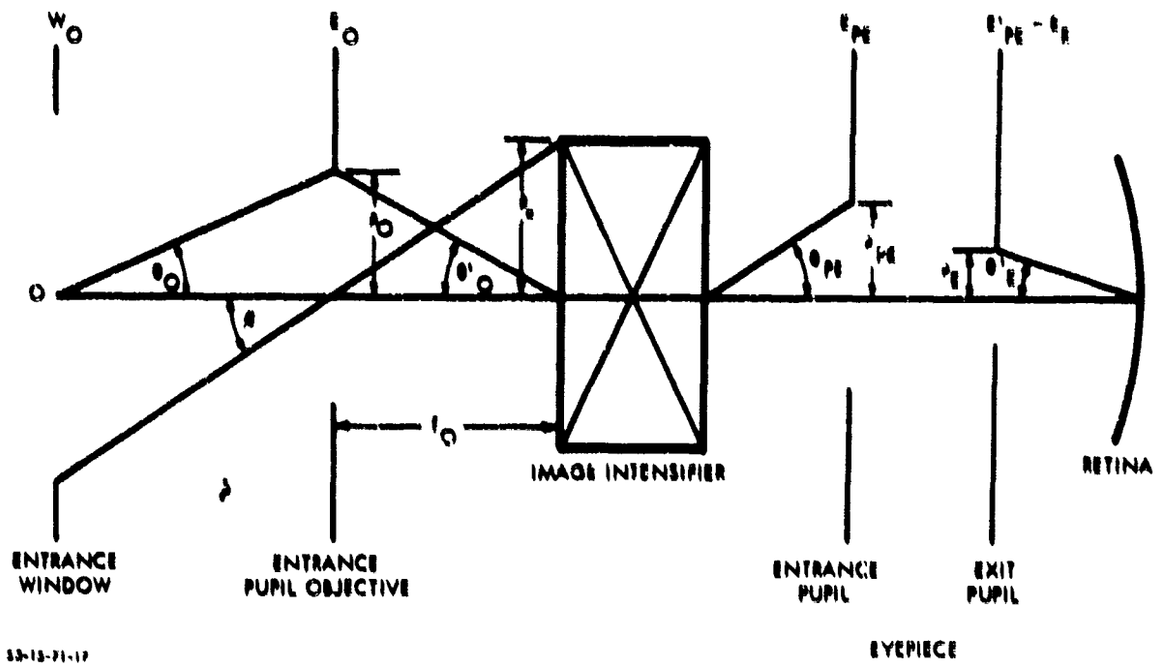


FIGURE 5. Schematic Diagram of Image-Intensifier Visual System

The magnification $m_u$ of the unaided eye viewing the same distant object is given by

$$m_u = (n/n')(\sin \theta_E/\sin \theta'_E) \qquad (16)$$

where $\theta_E$ and $\theta_E'$ are the angles subtended by the radius (the radii of entrance and exit pupils of the eye are nearly equal) of the eye pupil at the distant object and its image on the retina, respectively.

The subjective magnification M of the complete image intensifier system is by definition equal to the ratio of $m_B$ to $m_U$. Therefore, by combining Eqs. 13 through 16 with this definition and rearranging, $\mathfrak{m}$ is given by

$$\mathfrak{m} = m_I\ (\sin\theta_O/\sin\theta_E)(\sin\theta_{PE}/\sin\theta_O')(\sin\theta_E'/\sin\theta_{PE}'). \qquad (17)$$

For a distant object, $\sin\theta_O/\sin\theta_E \approx \rho_O/\rho_E$, and for a well-designed eyepiece, $\theta_E' = \theta_{PE}'$, since the eye pupil is the aperture stop. It is evident from Fig. 5 that

$$\sin\theta_O' = \rho_O'/(\rho_O'^2 + f_O^2)^{1/2} \qquad (18)$$

where $\rho_O'$ is the radius of the exit pupil and $f_O$ is the focal length of the objective. In terms of the f-number, Eq. 18 becomes

$$\sin\theta_O' = \left[1 + 4\ (f/no.)_O^2\right]^{-1/2}. \qquad (19)$$

Finally, the subjective magnification reduces to

$$\mathfrak{m} = m_I\ (\rho_O/\rho_E)\ \left[1 + 4\ (f/no.)_O^2\right]^{1/2} \sin\theta_{PE}. \qquad (20)$$

Examination of Eq. 20 reveals that, in contrast to binocular systems, image-intensifier systems can be designed to have as large an aperture as desired without a concomitant increase in $\mathfrak{m}$ by reducing either $m_I$ or $\sin\theta_{PE}$ to compensate for the increase in $\rho_O$. Consequently, the collection power of the system can be increased while the area

of the retinal image of an object is kept at a size sufficiently small for the eye to integrate the signal efficiently.

Equation 20 may be further reduced by expressing $\sin \theta_{PE}$ in terms of the subjective magnification $\mathfrak{m}_p$ of the eyepiece. By definition, $\mathfrak{m}_p = \mathfrak{m}_{PE}/m_u$ and, according to Eqs. 15 and 16, one has $\sin \theta_{PE} = \mathfrak{m}_p / \sin \theta_E$, where again one has assumed the eye pupil is the aperture stop, so that $\theta'_{PE} = \theta'_E$. In the standard definition of the subjective magnification of an eyepiece, it is assumed that the distance from the unaided eye to the object plane is 254 mm. Hence, $\sin \theta_E = \rho_E/254$, and $\sin \theta_{PE}$ is given by

$$\sin \theta_{PE} = \rho_E \mathfrak{m}_p/254. \tag{21}$$

If one substitutes Eq. 21 into Eq. 20 and neglects unity in comparison with $4\,(f/no.)_O^2$, one obtains

$$\mathfrak{m} = m_I(f_O/254)\mathfrak{m}_p. \tag{22}$$

The term $f_O/254$ may be considered to be the subjective magnification of the objective just as for the case of a visual telescope (Ref. 3). Likewise, by referring to Fig. 4 and the definition of $\mathfrak{m}_p$, it can be shown (Ref. 3) that $\mathfrak{m}_p = 254/f_p$, where $f_p$ is the focal length of the eyepiece. If one substitutes this expression for $\mathfrak{m}_p$ in Eq. 22, one obtains

$$\mathfrak{m} = m_I f_O/f_p. \tag{23}$$

This expression for $\mathfrak{m}$ differs from that for binoculars by the factor $m_I$, which, as shown above, allows adjustment of $\mathfrak{m}$ independent of the collection power.

The field of view of an image-intensifier system is determined by the photocathode, which acts as the field stop. Referring to Fig. 5, one notes that the total angular field of view is $2\beta$, where $\beta$ is determined by

$$\beta = \tan^{-1} (\rho_c/f_O) \tag{24a}$$

and $\rho_c$ is the radius of the photocathode. In terms of the f-number $(f/no.)_O$ of the objective, $\beta$ is given by

$$\beta = \tan^{-1} [\rho_c/2\ \rho_O\ (f/no.)_O]. \tag{24b}$$

The f-number of objectives is limited by technology to values greater than approximately unity. Hence, an increase in $\rho_O$ for greater collection efficiency must be accompanied by a commensurate increase in $\rho_c$ to maintain the same field of view independent of the subjective magnification.

In image-intensifier systems, if sufficient gain is provided, the appearance of a scintillation on the display will educe a visual sensation in the retina. Hence, the quantum efficiency of a visual system incorporating an image intensifier is characteristic of the quantum efficiency of the image-sensing surface of the intensifier. The photocathodes employed as image sensors in image intensifiers are discussed in Section IV-B.

If the duration of a scintillation produced on the display of an image intensifier is considerably longer than the integration time of the eye, the effective integration time of the complete visual system is characteristic of the integration time of the intensifier. Generally, however, image intensifiers are designed with integration times comparable to that of the eye to avoid loss of visual perception for moving targets.

2. Television Systems

Television systems for low-light-level applications offer some additional degrees of design flexibility not available to direct-view image-intensifier systems. Besides the possibility of separating the position of the image sensor from the image display, it is possible to perform contrast enhancement and other forms of image processing by means of associated optical and computer systems with the long-range

possibility of a completely automatic photoelectronic imaging and decision-making system.

These additional degrees of design flexibility in remote-view television systems result from the incorporation of an additional conversion process not found in direct-view image intensifiers--the conversion of the two-dimensional electron image generated at the primary photocathode into a video signal current by means of sequential readout of the image elements of the electron image on the camera-tube charge storage target. The conversion of the electron image into a video signal and subsequent amplification may introduce a limit on sensitivity not associated with the parameters of the eye. The minimum detectable signal current will be determined by the video preamplifier noise unless sufficient electron multiplication of the primary photoelectron is provided. In practice, it has been found that an electron multiplication of about $10^4$ is required. Electron multiplication may be achieved with image-intensifier modules and/or internal electron multiplication by means of electron bombardment of the storage target.

If sufficient electron multiplication ahead of the storage and readout system is provided, the video current will consist of a coarse-grained signal current of large pulses reflecting the Poisson distribution and its noise in the signal current--large pulses compared to the usual fine-grained noise current of the preamplifier. The luminous image formed on the display by conversion of the video current will consist of bright scintillations forming the image and a dim background randomly generated by the video noise current. Under these conditions, the quantum efficiency of the total visual system comprising the remote-view television system and the operator will be characteristic of the primary photocathode. Threshold sensitivity and integration time, as in direct-view image-intensifier systems, will be at the disposal of the designer subject to whatever restrictions are imposed by operational requirements, size, weight, and cost.

The same flexibility in design of subjective magnification and radiant flux collection power exists in remote-view television systems

as in direct-view image-intensifier systems. However, the subjective magnification is not so rigidly specified. The difference lies in the fact that the magnification between the display and the retina depends on the distance, which may not be rigidly controlled. If one follows the convention that normal magnification corresponds to a separation of 254 mm, then for a separation $S_D$ one has

$$\mathfrak{m}_p = 254/S_D \tag{25}$$

where $\mathfrak{m}_p$ is the subjective magnification between display and eye. Then, by Eq. 22, one has for the subjective magnification of a remote-view television system

$$\mathfrak{m} = m_I(h_D/h_T)(f_O/S_D) \tag{26}$$

where $m_I$ is the magnification between the primary photocathode of the intensifier stages and the camera-tube target, $h_D/h_T$ is the ratio of the heights of the display and target, respectively, and $f_O$ is the focal length of the objective.

The field of view of a television system, as determined by the size of the primary photocathode and the focal length of the objective, is given by Eq. 24, derived for image-intensifier systems.

## B. SPECTRAL RESPONSE OF PHOTOCATHODES

The effectiveness of a photocathode employed in a low-light-level photoelectronic imaging (PEI) system largely depends on the match between the spectral content of the input image irradiance and the spectral responsivity of the photocathode. The principal sources of passive nighttime radiant power in the order of decreasing magnitudes are the full moon, the hydroxyl emissions of the upper reaches of the atmosphere known as airglow, and the stars. The spectral content of moonlight, of course, is somewhat similar to that of sunlight. The airglow, whose integrated spectral radiant power (in the range from 0.6 to 1.8 microns) is only a factor of 10 less than full moonlight, exhibits

roughly an exponentially increasing spectral radiant power dependence on wavelength. In addition, since both the contrast of military targets against vegetation increases and the loss of contrast in transmission via atmospheric scattering decreases with increasing wavelength from the visible into the near infrared, it is valuable in low-light-level PEI systems to employ photocathodes with high near-infrared response.

The spectral responses of several typical photocathodes used as image sensors in PEI systems are shown in Fig. 6. The S-1 surfaces are sensitive well into the near infrared and have been used in conjunction with auxiliary near-infrared scene irradiators designed to achieve operational covertness. One application during World War II was the sniperscope. Although the S-10 surface has been used extensively in commercial broadcast applications, where the similarity between its spectral response and that of the eye (shown in Fig. 1) is prized, it is of no interest in the design of low-light-level PEI systems. The S-20 and its derivatives, the S-25 and S-20VR*, with their high responsivity in both the visible and near-infrared portions of the spectrum, are the standard photocathodes employed in low-light-level PEI systems.

The responsivity $\sigma(\lambda)$ of a photocathode at a wavelength $\lambda$ in amperes per watt is given by

$$\sigma(\lambda) = \lim_{\Delta\lambda \to 0} [j_s/H_\lambda \Delta\lambda] \tag{27}$$

where $j_s$ is the value of the photoelectric current density produced by irradiance within the wavelength interval $\Delta\lambda$, and $H_\lambda$ is the spectral irradiance at a wavelength in the interval $\Delta\lambda$.

---

*S-20VR is not a Joint Electron Device Engineering Council (JEDEC) term but is applied to the recent better S-20 cathodes by Varo, Inc., and others.

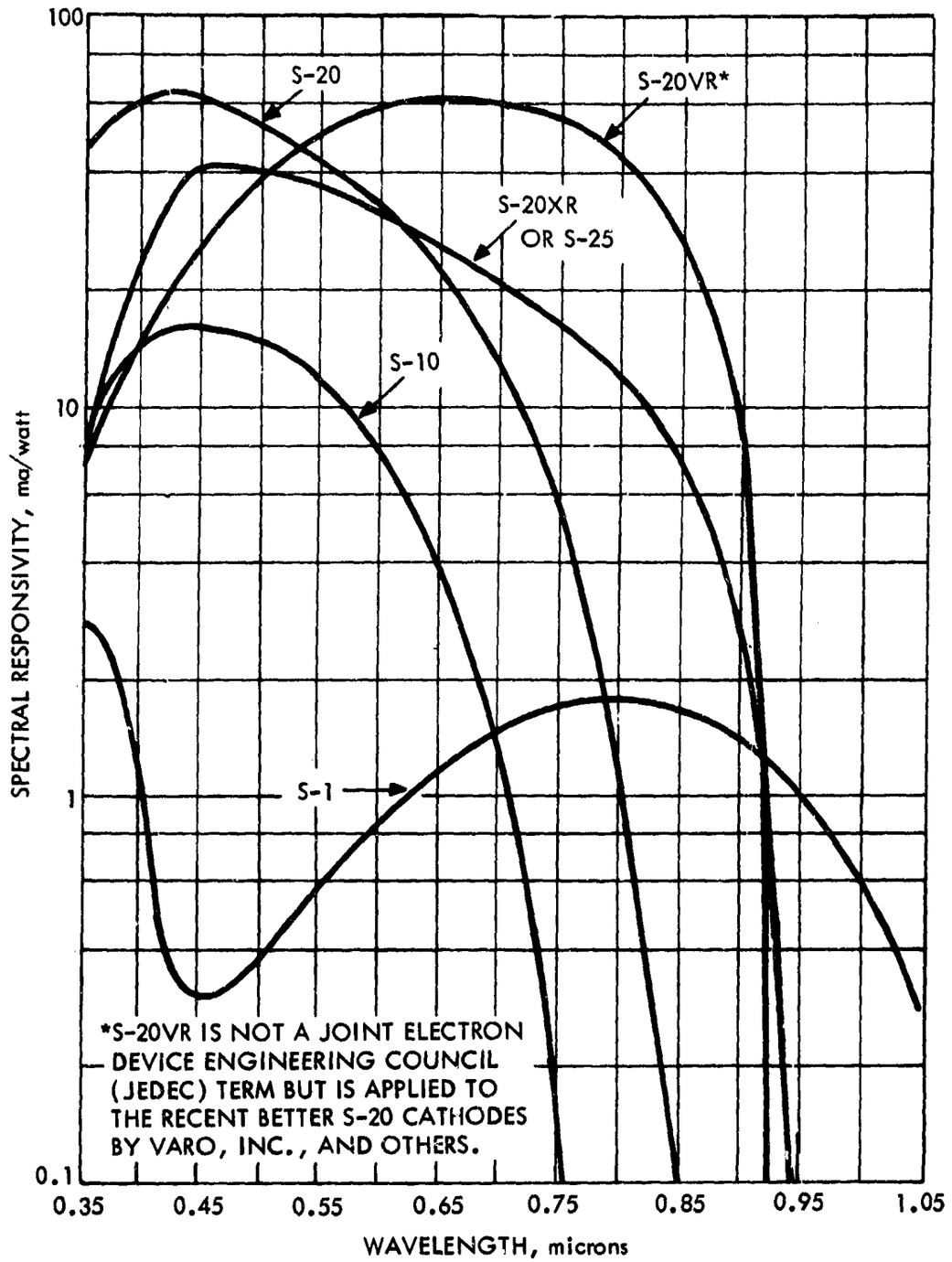


S3-15-71-15

FIGURE 6. Spectral Responsivity Versus Wavelength for Several Photoemissive Photocathodes

The performance of a photocathode irradiated by a source of spectral composition described by $H_\lambda$ is measured by the total photoelectric current density produced by the total irradiance. Analytically, it is given by

$$j_s = \int_0^\infty \sigma(\lambda) H_\lambda d\lambda \tag{28a}$$

or

$$j_s = \sigma(\lambda_p) \int_0^\infty R(\lambda) H_\lambda d\lambda \tag{28b}$$

where $\sigma(\lambda_p)$ is the peak value of the responsivity at the wavelength $\lambda_p$ of the peak, and the dimensionless function $R(\lambda)$ is the relative value of the responsivity function of $\lambda$.

Often the mean responsivity $\sigma$ is specified as a measure of the quality of a photocathode. The mean responsivity is defined by

$$\sigma = \frac{\int_0^\infty \sigma(\lambda) H_\lambda d\lambda}{\int_0^\infty H_\lambda d\lambda} \tag{29}$$

which is equivalent to

$$\sigma = j_s/H$$

where $H = \int_0^\infty H_\lambda d\lambda$ is the total irradiance. Thus, the performance of a photocathode with a source of irradiance of a given spectral composition may be specified equally well by the value of $j_s$ at a given value of H or by $\sigma$.

It is important to note from Eq. 29 that $\sigma$ depends on the spectral composition of the irradiance as well as the spectral dependence of the responsiviity itself. Thus, it is necessary to make sure, in comparing the responsivities of different photocathodes to be used with a given source, that the responsivities were determined with the same given source or one of similar spectral composition.

Unfortunately, a variety of standard sources, matching natural sources such as moonlight and airglow, is not available for measuring the mean responsivity of photocathodes. Only the tungsten lamp at $2854^{o}K$ has been accepted as a standard source. The mean responsivity $\sigma_T$ of a photocathode measured with this source is given by

$$\sigma_T = \frac{\int_0^\infty \sigma(\lambda) H_{\lambda,\ 2854^{o}K}\, d\lambda}{\int_0^\infty H_{\lambda,\ 2854^{o}K}\, d\lambda} \tag{30}$$

where $H_{\lambda,\ 2854^{o}K}$ is the spectral irradiance due to the tungsten lamp operated at $2854^{o}K$ in watts per micron-meter squared.

The value of the mean responsivity $\sigma_T$ of an S-10 surface measured with a $2854^{o}K$ lamp is typically 0.8 ma/watt.

One of the first steps forward in low-light-level imaging was the development of the S-20 surface with a $\sigma_T$ of typically 3 ma/watt. This surface was gradually improved by extending its red response so that by the mid-1960's values of $\sigma_T$ equal to 4 ma/watt became quite commonplace, with occasional values as high as 5 to 6 ma/watt. As the S-20 was improved, it became known as the S-20XR (XR for extended red) and was finally type-classified as the S-25. More recently even further improvements have resulted in a surface which is tentatively described as the S-20VR (VR for very red), whose mean responsivity is reported to vary from 5 to 9 ma/watt. The responsivity of the S-20VR in the near infrared is especially notable. Both the S-25 and the

S-20VR will be used in calculations, although the S-20VR is not now as commonly available.

If the thermionic emission or dark current of a photocathode is comparable to or higher than the photoelectric current, contrast in the output image of a scene is reduced. The thermionic emission or dark current of the S-1 is quite high, being $10^{-11}$ to $10^{-12}$ amp/cm$^2$ at room temperature. In many cases it is necessary to cool this surface to avoid excessive contrast loss. The dark current of the S-10 is considerably better at $10^{-13}$ to $10^{-14}$ amp/cm$^2$ but is still higher than desired for low-light-level applications. For the S-20 and S-25 surface, dark current is extremely low ($10^{-15}$ to $10^{-16}$ amp/cm$^2$) and is not ordinarily a problem. The dark current of the S-20VR is similarly low.

## C. LUMINOUS CONVERSION FACTOR OF PHOSPHORS

In the operation of a low-light-level PEI system, the photoelectric current density generated at the primary photocathode is first amplified and then focused onto an output phosphor where a radiant image is generated with spectral radiance $L_\lambda(\lambda)$ given by

$$L_\lambda(\lambda) = j_D k_{\lambda D}(\lambda) \tag{31a}$$

or

$$L_\lambda(\lambda) = j_D k_{\lambda D}(\lambda_p)\, Z(\lambda) \tag{31b}$$

where $j_D$ is the current density incident on the phosphor, $k_{\lambda D}(\lambda)$ is the spectral radiant conversion factor of the phosphor in watts per nanometer-steradian-ampere, $k_{\lambda D}(\lambda_p)$ is the peak value of $k_{\lambda D}$ at the wavelength $\lambda_p$ of the peak, and the dimensionless function $Z(\lambda)$ is the relative value of the spectral radiant conversion factor. For a given set of electrode potentials the spectral radiant conversion factor of an image intensifier or kinescope is constant over a range of incident

current densities $j_D$ from near zero to near a saturation value. The saturation current density of zinc sulphide phosphors such as the P-20 is approximately 0.1 ma/cm$^2$, independent of the incident electron energy.

The relative spectral radiant conversion factor as a function of $\lambda$ is shown in Fig. 7 for the typical modified P-20 phosphor used in most modern image-intensifier tubes. Comparison of the spectral radiant conversion factor of the modified P-20 with the relative spectral response curve of the eye shown in Fig. 1 and the photocathode spectral responsivity curves shown in Fig. 6 reveals that efficient optical coupling exists between this phosphor and both the human eye and the photocathodes S-20 and S-25.

The luminous conversion factor $k_{L'B}$ of a PEI system is defined by $k_{L'B} = B_D/L'$, the ratio of the luminance $B_D$ of the output phosphor to the "apparent" radiance $L'$ of the scene. (If the atmospheric transmission were unity or the distance to the scene were small, $L'$ would be the radiance of the scene.) The units of $k_{L'B}$ reduce from (candela/meter$^2$)/(watt/meter$^2$-steradian) to simply lumen/watt.

The dependence of the phosphor luminance on the apparent radiance of the scene is given by

$$B_D = K_D \left[ \int_0^\infty k_{\lambda D}(\lambda)\, d\lambda \right] \left( G_I/m^2 \right) \sigma \left[ \pi L'/4(f/no.)^2 \right] \qquad (32)$$

where the last bracketed factor is the input irradiance $H_S$ to the photocathode, $\sigma H_S$ is the photoelectric current density $j_s$ generated at the photocathode, $(G_I/m^2)\, j_s$ is the photoelectric current density $j_D$ incident on the output phosphor ($G_I$ is the electric current gain, m is the magnification), the product of the first bracketed term and $j_D$ is the radiance of the phosphor, and

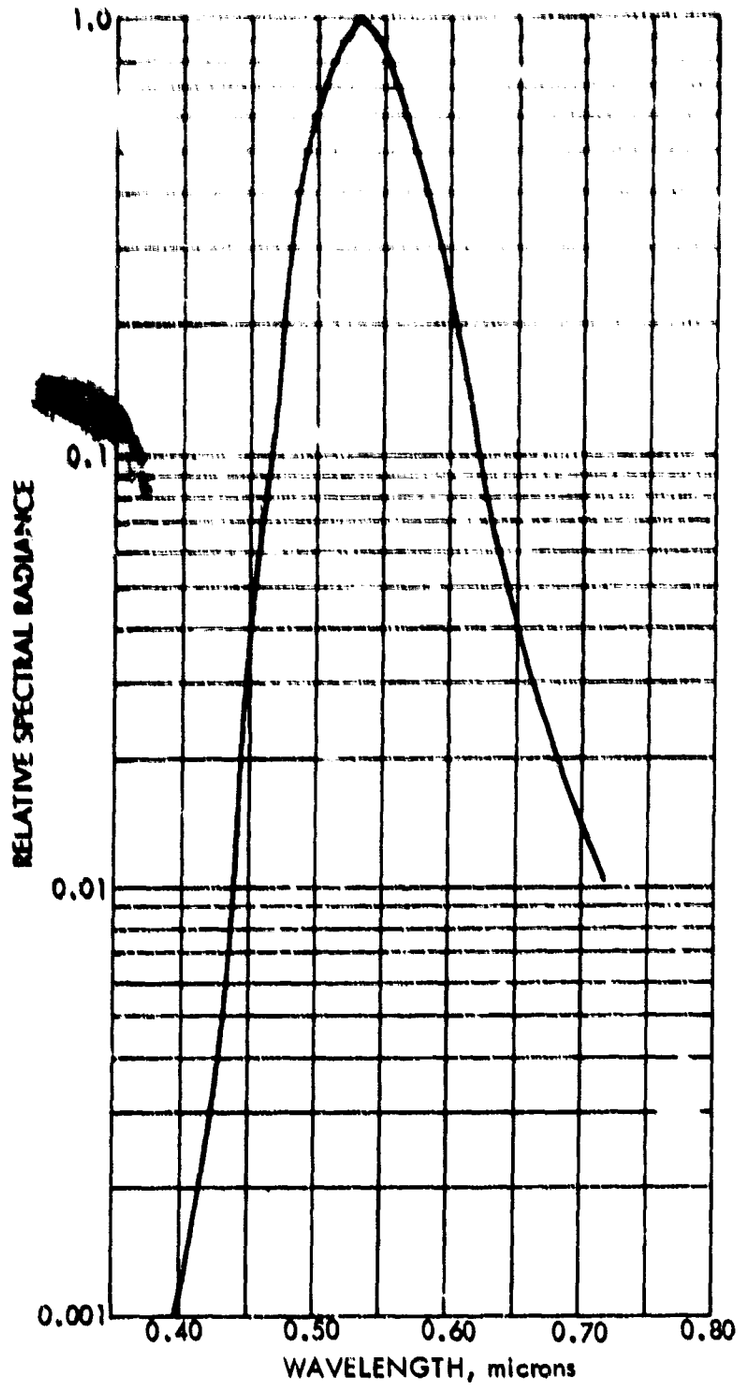


FIGURE 7. Relative Spectral Radiance of a Modified P-20 Phosphor

$$K_D = 680 \int_0^\infty y(\lambda) k_{\lambda D}(\lambda)\, d\lambda \Big/ \int_0^\infty k_{\lambda D}(\lambda)\, d\lambda \tag{33}$$

is the luminous efficacy of the output radiance.

It is convenient to express Eq. 32 in the following form

$$B_D = \pi k_{HB} \eta_C L' \tag{34}$$

where $k_{HB} = B_D/H_S$ is the luminous conversion efficiency of the PEI device and $\eta_C = 1/4(f/no.)^2$ is the collection efficiency of the objective (for a perfectly transmitting atmosphere and diffusively reflecting object $\eta_C$ is the ratio of the photocathode irradiance to the object irradiance). The units of $k_{HB}$ are (candela/meter$^2$)/(watt/meter$^2$), which reduce to lumen/watt-steradian. Tables including values of $k_{HB}$ for several image-intensifier tubes are presented in Part IV of Ref. 8.

In terms of $k_{HB}$ and $\eta_C$ the luminous conversion factor of a PEI system according to Eq. 34 is given by

$$k_{L'B} = \pi k_{HB} \eta_C \tag{35}$$

and by Eq. 32 the luminous conversion factor of a PEI device is given by

$$k_{HB} = K_D \left[\int_0^\infty k_{\lambda D}(\lambda)\, d\lambda\right] \left(G_I/m^2\right) \sigma. \tag{36}$$

If the phosphor is a Lambertian radiator or, if not, within the approximation that it is, the power gain defined by the ratio of radiant power emitted by the phosphor to radiant power incident on the photocathode is given by

$$G_p = \pi(L_D/H_S)\ m^2 \tag{37a}$$

or

$$G_p = \pi G_I \sigma \int_0^\infty k_{\lambda D}(\lambda)\, d\lambda \tag{37b}$$

where the only new symbol in the above equations is $L_D$ equal to the radiance of the phosphor. Gain factor $G_p$ is dimensionless, as is any gain factor. In terms of $G_p$, the luminous conversion factor of a PEI system is given by $k_{HB} = k_D G_p \eta_C/m^2$, and the luminous conversion factor of a PEI device is given by $K_{HB} = K_D G_p/\pi m^2$. It should be noted that the luminous conversion factors and power gain defined above depend on $\sigma$, which was defined in Section IV-B and shown to depend on both the spectral distribution of the source and the spectral dependence of the responsivity.

The ratio of the luminance of the output phosphor in footlamberts to the illuminance of the photocathode in footcandles has been widely employed as the definition of the "brightness" gain $G_B$ of an image intensifier tube. The above units of $G_B$ reduce to ($\pi$ steradians)$^{-1}$. However, if the phosphor can be approximated by a Lambertian radiator, then $G_B$ can be considered to be dimensionless--equal to the ratio of the luminous exitance of the phosphor in lumen/ft$^2$ to the illuminance of the photocathode in footcandles. The expression for the "brightness" gain is given by

$$G_B = \pi k_{HB}/K_S \tag{38}$$

where $k_{HB}$ is given by Eq. 36 and $K_S$, the luminous efficacy of the input irradiance, is given by

$$K_S = 680 \int_0^\infty y(\lambda)\, H_{\lambda S}(\lambda)\, d\lambda \Big/ \int_0^\infty H_{\lambda S}(\lambda)\, d\lambda \tag{39}$$

where $H_{\lambda S}(\lambda)$ is the spectral irradiance function of wavelength $\lambda$ at the photocathode. The factor $\pi$ in Eq. 38 arises from the fact that the unit solid angle in the definition of $G_B$ is $\pi$ steradians.

The use of "brightness" gain as a characteristic parameter of an image-intensifier tube is to be strongly discouraged for the following reasons:

- The proper units (Ref. 1) for luminance and illuminance are candela/meter$^2$ and lumen/meter$^2$, respectively (not footlambert and footcandle).
- The use of luminous units for the input to a photocathode is often misunderstood, for although a lumen of luminous power from any source produces the same visual response, the response of a photocathode depends on the spectral content of the luminous power.
- Photocathodes used in image-intensifier tubes exhibit infrared responsivity, so that an output luminance may result even if the luminous efficacy of the input irradiance is zero.

In the latter event the "brightness" gain given by Eq. 38 would be undefined. Instead of "brightness" gain the luminous conversion factor $k_{HB}$ is preferred.

It has been standard practice to measure the "brightness" gain with a 2854$^{\circ}$K tungsten lamp. The luminous efficacy of radiant power from this standard source is approximately 20 lumen/watt. Hence, according to Eq. 38 measurements of $G_B$ with a 2854$^{\circ}$K tungsten lamp may be converted to the luminous conversion factor by the formula $k_{HB} = 20G_B/\pi$.

The luminous conversion factor of two image-intensifier tubes in cascade is given by Eq. 36, where the output phosphor is that of the second tube, the photocathode is that of the first tube, and the current gain $G_I$ results from coupling the radiant power generated at the first phosphor to the photocathode of the second tube. Thus, in a two-stage image intensifier (without an electron multiplication dynode),

the current gain defined by $G_{I12} = j_{s2}/j_{D1}$ is given approximately by

$$G_{I12} = \pi\eta_T \int_0^\infty \sigma_2(\lambda)\, k_{\lambda D1}(\lambda)\, d\lambda \tag{40a}$$

or equivalently by

$$G_{I12} = \pi\eta_T\sigma_2\left(\lambda_p\right) k_{\lambda D1}\left(\lambda_p\right) \int_0^\infty R_2(\lambda)\, Z_1(\lambda)\, d\lambda \tag{40b}$$

where the subscripts 1 and 2 refer to the first and second stages, respectively, and $\eta_T$ is the transfer efficiency of the radiant power from the first phosphor to the second photocathode. The value of $G_{I12}$ is usually in the range 30-50 with 40 being a typical value for image-intensifier tubes with a P-20/S-20 phosphor-photocathode combination.

## D. TEMPORAL RESPONSE

If an image system has a temporal response longer than that of the eye, the effect is to smear together image detail when an input image moves across the photocathode. In an intensifier some lag due to phosphor decay can be expected. One such measurement of temporal response performed with a modulated light source is shown in Fig. 8. The temporal response at the normal TV frame rate (30 frames/sec) is seen to be quite high for a single-stage intensifier but is appreciably lower for three-stage intensifiers. Methods of measuring and specifying temporal responses are not well known, but such measurements and specifications can be quite important, and are discussed in connection with TV camera tubes in Ref. 8.

Although intensifiers do exhibit lag effects of their own, their addition to a system can reduce overall system lag. Most camera tubes, in particular, have lag characteristics that depend on light level. That is, lag increases as light level decreases. By increasing light

level on the camera tube, the increase in lag due to an added intensifier is usually more than offset by the decrease in camera lag.

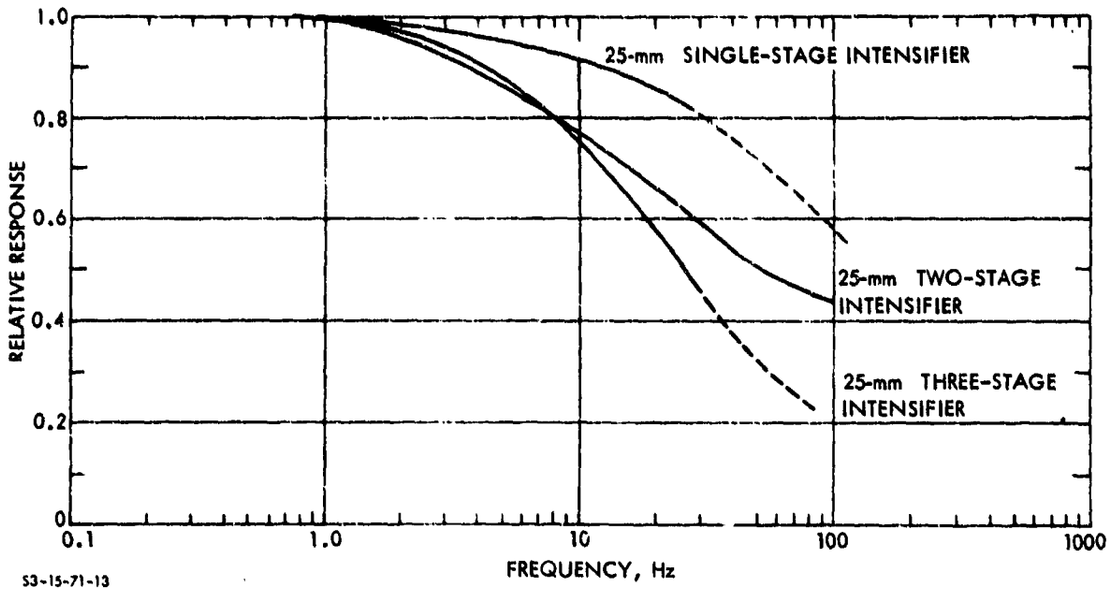


FIGURE 8. Temporal Response of Image Intensifiers

E. SPATIAL FREQUENCY RESPONSE, MODULATION TRANSFER FUNCTION

In the process of detecting the input image, converting it into electrons, focusing it onto the phosphor, and recreating a visible image, contrast is lost at each step for the reason that aberrations cause an overlapping of the radiance pattern on the display produced by the input image irradiance. In the limit of small-image element sizes, as contrast falls below a few percent, detection probability approaches zero.

Rather than reproduction of contrast on the display as a function of image element size, it is customary to consider the reproduction of

the modulation amplitude of a sinusoidal, spatially modulated, radiant test pattern as a function of spatial frequency. The relation between contrast and modulation amplitude is described below. The modulation transfer function (MTF) or sine-wave response of a PEI system is defined as the ratio of the modulation amplitude of the display image to the modulation amplitude of the input image on the photocathode as a function of spatial frequency--normalized to unity as the frequency approaches zero. The sine-wave response can be measured by projecting a sine-wave pattern with 100 percent modulation onto the photocathode. First, a sine-wave pattern of low spatial frequency is employed and the peak-to-peak output amplitude is noted. With this amplitude as a reference, the pattern spatial frequency is increased in discrete steps. At each step, the new peak-to-peak amplitude is measured and the ratio of this amplitude to that measured at the low spatial frequency is formed. The plot of these amplitude ratios as functions of pattern spatial frequency constitutes the sine-wave response.

The sine-wave spatial frequency is described quantitatively in terms of $\nu$, the number of cycles (or line pairs) per millimeter or, alternatively, the number of half cycles (or lines) in some dimension such as the photocathode diameter or height of the display. The sine-wave responses of a typical single-intensifier module and of two- and three-intensifier modules, respectively, in cascade with unity magnification are shown in Fig. 8. In general, the overall sine-wave response of several components in cascade is given by

$$T(\nu_{1s}, \nu_{nD}) = T_1(\nu_{1s}/m_1)T_2(\nu_{1s}/m_1m_2)\ldots T_n(\nu_{1s}/m_1m_2\ldots m_n) \qquad (41)$$

where $T(\nu_{1s}, \nu_{nD})$ is the overall sine-wave response on the output phosphor at frequency $\nu_{nD}$ to an input sine-wave pattern at frequency $\nu_{1s}$; $T_1(\nu_{1s}/m_1)$ is the sine-wave response of the first component, etc.; $m_1$ is the image magnification in the first component, and so on. Equation 41 results from observing that:

- The spatial frequency on the display is related to the spatial frequency on the sensor by $\nu_D = \nu_s/m$.

- The modulation amplitude M at the input to the second component is equal to the modulation amplitude at the output of the first component.
- The modulation amplitude at the output of each component is related to the modulation input by $M_D = T(\nu/m)M_S$.

It is apparent, on referring to Fig. 9, that care must be exercised in cascading components that the expected increase in performance due to increased intensifier gain at the designed spatial frequency is not cancelled by the reduced sine-wave response of cascaded stages at that spatial frequency.

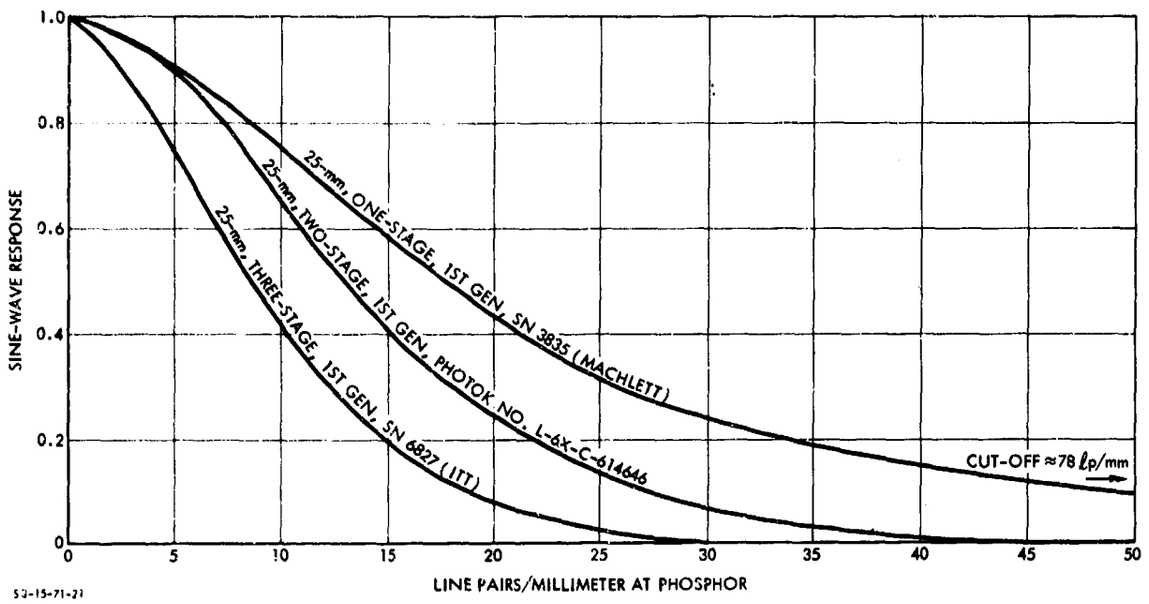


FIGURE 9. Modulation Transfer Function of Image Intensifiers

The case of a zoom intensifier merits special attention. If the zoom-intensifier sine-wave response were unity at all spatial frequencies, resolution would be unlimited in both wide-angle and narrow-angle modes. Since the wide-angle mode also covers more viewfield, there would be little point to zoom with consequent reduction of viewfield. As a practical matter, the sine-wave response of the intensifier

is limited by aberrations in the electron optics and the phosphor particle sizes. The sine-wave response of a zoom intensifier in both wide- and narrow-angle modes is shown in Fig. 10. As the viewfield is decreased, going from the wide- to the narrow-angle modes, image magnification increases from $m_W$ to $m_N$ in the same ratio. Consequently, the spatial frequency scale of the sine-wave response curve is compressed by the factor $m_N/m_W$ or, alternatively, on the same frequency scale the abscissa of points on the curve may be multiplied by $m_N/m_W$, shifting the entire curve as indicated in Fig. 10. Specifically, for an 80/25-mm zoom tube, the magnification increases from approximately 1/3 to unity as the viewfield is decreased, and the abscissa of points on the wide-angle curve at a given response is shifted in the narrow field mode by approximately three times the frequency. Thus, some of the higher sine-wave response at a given target spatial frequency in the narrow-angle mode is sacrificed in the wide-angle mode for the sake of wider viewfield. On the other hand, greater brightness gain is realized and, if sufficient brightness gain is not otherwise provided, may provide some improvement in performance.

For evaluation of the overall performance of a complete visual system comprising both the human operator and the PEI system, it is also necessary to consider the spatial frequency response of the eye and the relation between frequency on the display and on the retina. Since it is not feasible to monitor the spatial dependence of the electrical signals generated in the eye as a function of spatial variations in the irradiance of the retina, it is not possible to make a direct measurement of the spatial frequency response. Rather, spatial frequency response can only be indirectly inferred from measurements of the modulation amplitude of a sine-wave test pattern required by the eye for some specified detection probability and the signal-to-noise ratio theory of detection probability. The dependence of detection probability on the signal-to-noise ratio at the decision centers of the brain, because it involves such parameters as the quantum efficiency and the temporal and spatial bandwidths of the eye, is incomplete. However, the required modulation function alone is sufficient

to make predictions of the overall performance of a PEI system and its operator.

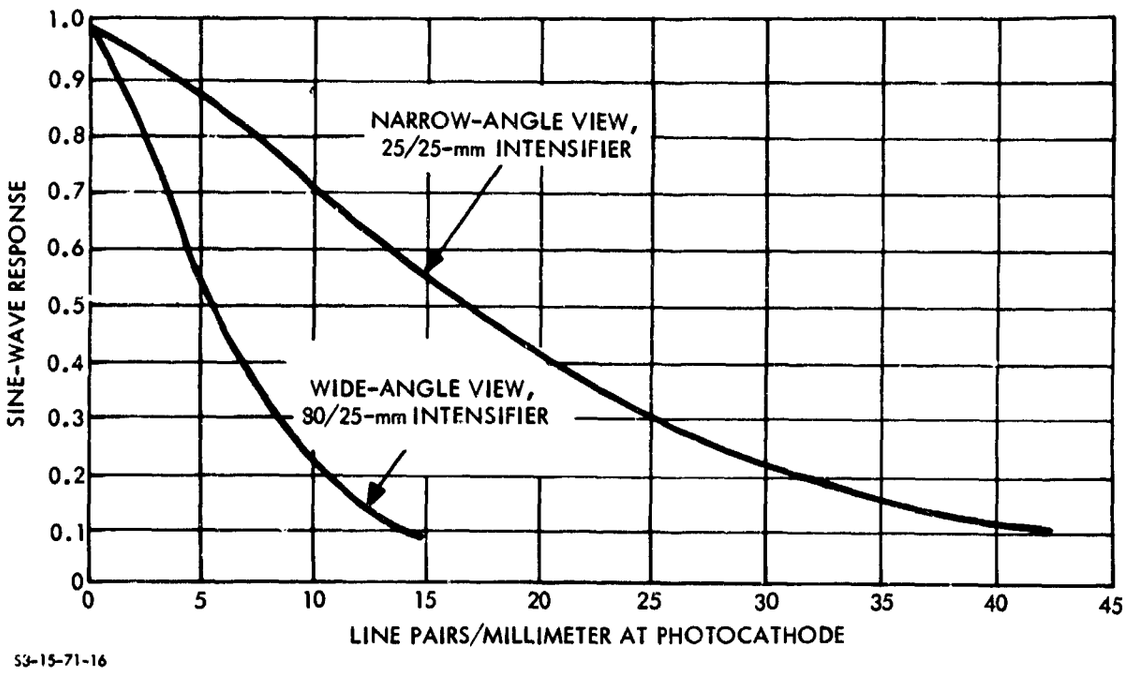


FIGURE 10. Response of a Zoom Intensifier Referred to the Input Photocathode

The frequency scale of the required modulation function depends on the distance from the eye to the display of a television monitor or the subjective magnification ($\mathfrak{m}$) of an eyepiece. If 254 mm (10 in.) is assumed as the standard viewing distance ($\mathfrak{m}$=1), then the relation between frequency $\nu_R$ on the retina and frequency $\nu_D$ on the display is given by

$$\nu_D = 0.067\mathfrak{m}\nu_R \tag{42}$$

where the separation of the retina and second nodal point of the eye

is assumed equivalent to 17 mm in air. For example, if the viewing distance were 30 inches, $\mathfrak{m}$ would be 1/3.

The required modulation as a function of frequency in cycles per inch calculated from retinal modulation sensitivity curves published by A. van Meeteren (Ref. 9) is shown in Fig. 11 for a subjective magnification of unity and three luminance levels. These curves were determined under conditions such that for a given display luminance the signal-to-noise ratio is maximum and hence, as will be explained in Section V, the curves represent the minimum required modulation functions. The curve at 0.52 cd/m$^2$ or 0.15 ft-L corresponds approximately to the usual luminance working level of an image-intensifier display. Figure 11 reveals that reduction of display luminance below 0.52 cd/m$^2$ has a dramatic effect on the required modulation function, while increases in display luminance have a much smaller relative effect.

The relation between the minimum required modulation functions and the output modulation of a typical low-light-level television system is shown in Fig. 12a and b at two display luminances, as indicated. The relation between frequency N in television lines per raster height and frequency $\nu_D$ for $\mathfrak{m}$=1 is given by

$$N = 20\nu_D/(S/H), \text{ for } \nu_D \text{ in cycles per inch,*} \tag{43a}$$

or

$$N = 500\nu_D/(S/H), \text{ for } \nu_D \text{ in cycles per millimeter,} \tag{43b}$$

where S is the separation between display and observer, and H is the raster height. In Fig. 12a and b, for 30 percent input modulation, the output modulation of a single-stage noise-free but otherwise typical low-light-level television tube as a function of spatial frequency is shown in conjunction with the required modulation at viewing

*Display tubes are normally measured in inches.

distances equal to six and three times the raster height. The frequencies at the intersections of the required modulation and output modulation curves are the resolution values of the eye-display combination under the assumed conditions. In Fig. 12b, increasing the viewing distance from three to six times the raster height reduces the resolution from roughly 500 to 350 television lines per raster height.

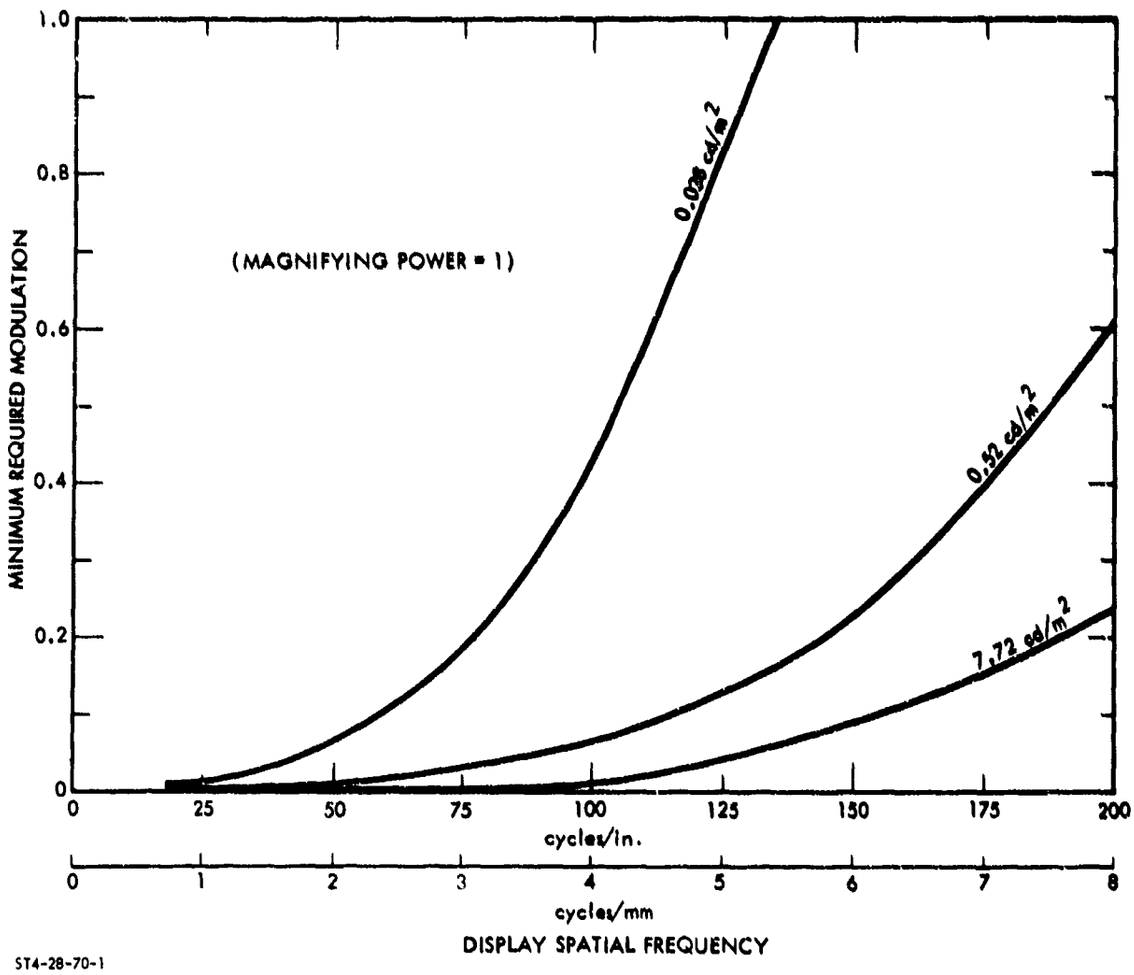


FIGURE 11. Minimum Required Modulation for Detection of Sine-Wave Pattern by Eye (Ref. 9)

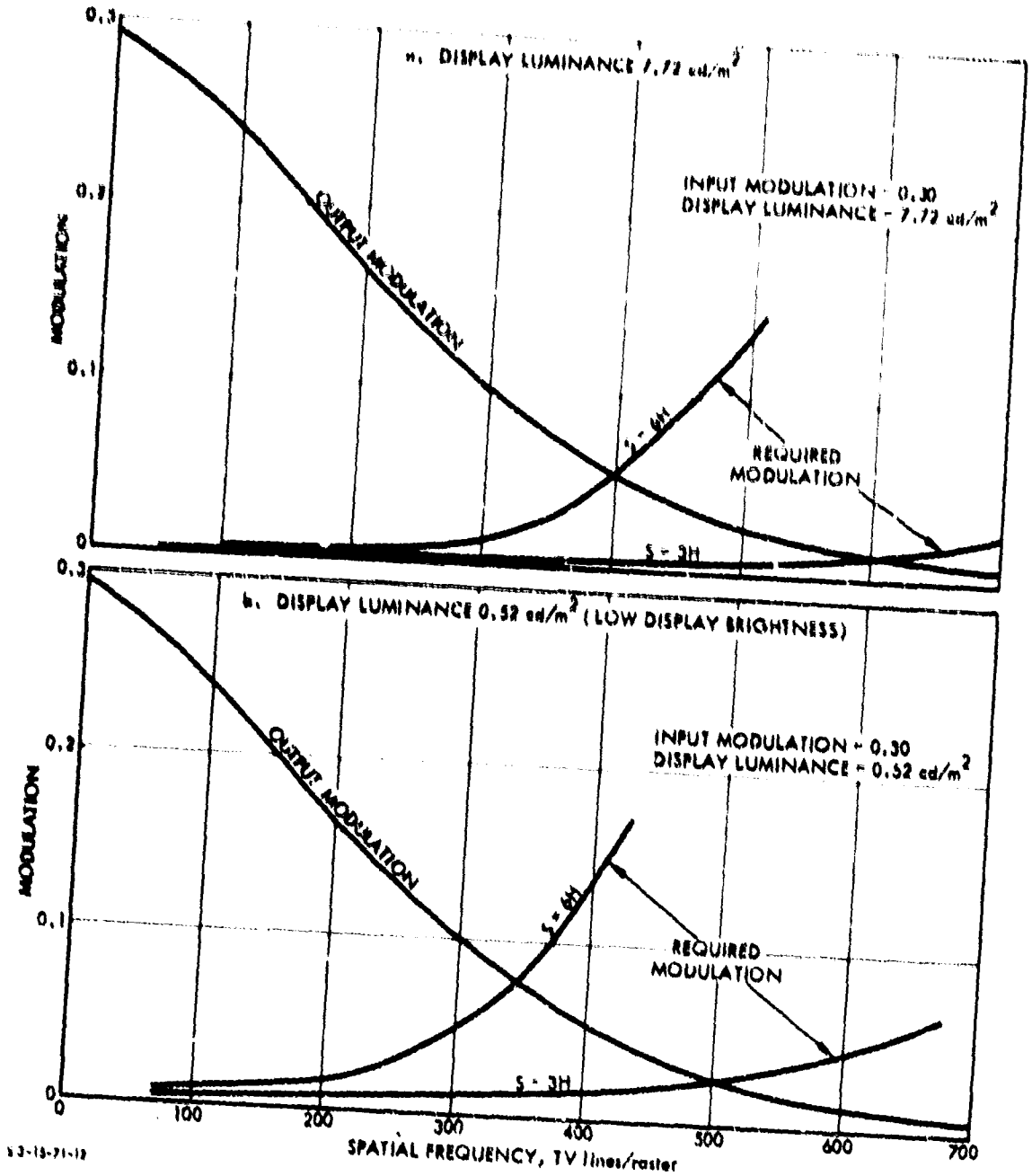


FIGURE 12. The Ultimate Limit for Visibility as a Function of Brightness and Viewing Distance. (Output Modulation for 30 Percent Input Modulation to a Noise-Free but Otherwise Typical Low-Light-Level Television Tube and Required Modulation for Viewing Distance S Equal to Six and Three Times Raster Height H. The Noise Level for the Data is Determined Only by the Electric Noise Generated in the Eye Due to the Photon Nature of the Display Luminance.)

In image-intensifier systems the subjective magnification of the eyepiece is typically seven times, which is equivalent to a viewing distance of only 1.4 in. Therefore, both the required modulation of the eye and the resolution are determined by the output luminance fluctuations considered in Section V. However, an exception may arise in single-stage demagnifying image intensifiers, where both M and the display luminance may become low compared to their corresponding values in a conventional multistage image intensifier.

It is important in the design of both remote-view television and direct-view image-intensifier systems to present the output image to the eye at sufficient luminance and angular size that the required modulation is little affected by the optical properties of the eye and the neurological organization of the retina but rather by the fundamental effects of output luminous fluctuations on the decision process discussed in Section V.

It has been determined empirically (Part II of Ref. 8) that excellent correlation exists between the subjective quality of aerial photographs and the modulation transfer function area (MTFA) bounded by the ordinate axis, the image modulation function of the photograph, and the required modulation function of the eye. The rationale for the choice (Ref. 10) of the MTFA as an overall measure of picture quality and observer performance is based on the observation that easy detection of a particular spatial frequency requires that the modulation should be as high as possible (conspicuous) above that required by the eye, for, say, 50 percent detection probability with unlimited viewing time. In aerial photographs, all spatial frequencies are generally of interest. Hence, the MTFA was proposed as an overall measure of observer performance and picture quality. In the visual observation of photographs, the modulation required by the eye at low spatial frequencies depends on the properties of the visual system. At higher spatial frequencies, fluctuations in grain size set the requirement and cause the required modulation to rise.

In the case of low-input image irradiance to PEI systems, a rise in required modulation with increasing frequency is observed that is

due to fluctuations in the output luminance produced by scintillations on the display. While the required modulation function depends on the optics and neurological organization of the eye at high input irradiance, at low-input irradiance the required modulation function is largely determined by the effects of luminance fluctuations at the display on the decision process. A different required modulation curve occurs at low-input irradiance for each photocathode at each input irradiance. The effect of fluctuations on the required modulation function of the eye is discussed in detail below.

## V. ANALYSIS OF PHOTOELECTRONIC IMAGING SYSTEMS

The probability of correctly identifying a known signal in the presence of noise is a function of the signal-to-noise ratio. It has been demonstrated by Rose (Ref. 6), Schade (Ref. 11), Coltman (Ref. 12), and Coltman and Anderson (Ref. 13) that the probability of detecting simple targets, such as disks on a uniform background, bar patterns, and sine-wave patterns, depends on the signal-to-noise ratio of the image formed on the display. They concluded that in an image formed by scintillations (under low brightness conditions when fluctuations in intensifier gain and internal sources of noise can be neglected), the signal is proportional to the average difference in the number of scintillations generated at adjacent image elements per sampling time (the effective integration time of the eye), and the noise is proportional to the root-mean-square value of the fluctuations in the difference.

The primary source of noise at the input of a PEI system arises from shot noise inherent in the photoelectric current generated at the photocathode by random absorption of the incident photon flux. It is observed that the numbers arriving on a small area of the sensor in equal intervals of time obey the Poisson distribution function. The root-mean-square value of the fluctuations about the average number is equal to the average number. Such temporal fluctuations constitute noise that inhibits image perception and reduces detection probability per glimpse.

For a given input-image element size and sampling time, the signal-to-noise ratio of the output image is determined by four properties of the PEI system:

**Preceding page blank**

1. The size of the entrance pupil of the objective.

2. The quantum efficiency of the photocathode.

3. The internal generation of noise, such as shot noise in thermionic current (fluctuations in electron multiplication processes and Johnson noise in the input resistor of the video amplifier).

4. The degree to which the input image can be reproduced on the display without overlap of the luminance of adjacent image elements, i.e., the modulation transfer function.

In image-intensifier tubes, thermionic current and fluctuations in electron multiplication are generally negligible compared to the shot noise of the photocathode current. In low-light-level television systems, if high intensifier gain is provided, the video amplifier output current consists of a coarse-grained current of large pulses and a fine-grained noise current. The large pulses result from charge pulses evoked by emission of an electron from the photocathode and by electron multiplication increased to several thousand electrons before the video amplifier. The fine-grained noise current in tubes without electron multipliers largely results from random thermal generation in the first stage of the video preamplifier. Intensification of a primary photoelectron by a factor of approximately $10^4$ at standard scan rates is sufficient to overcome the effect of video noise in the output image.

As an example, if the storage target comprises $5 \times 10^5$ storage elements and the frame time is 1/30 sec, the readout time of one storage element is $6.7 \times 10^{-8}$ sec. For a readout time of $6.7 \times 10^{-8}$ sec and primary electron intensification of $10^4$, the average pulse current due to a single photoelectron will be roughly 24 na, providing an average pulse-current signal-to-video-amplifier-noise ratio of 10 at the input to a good video preamplifier. Primary electron intensification of $10^4$ can be easily obtained with a combination of a one-stage image intensifier and SEBIR tube, can be just barely obtained with a one-stage image intensifier and SEC vidicon combination, and cannot be

realized with a double image intensifier and plumbicon or vidicon combination. The required factor of $10^4$ requires three cascaded intensifiers for an intensifier vidicon camera. However, more intensification, at a sacrifice in frequency response, is obtained by cascading more intensifier stages.

## A. NOISE-EQUIVALENT MODULATION

The following noise calculations apply to image-intensifier systems and to television systems possessing sufficient intensifier gain to make the effect of video amplifier noise in the output image negligible. The steps to be followed are to calculate the signal and the noise, form the S/N ratio, set it equal to unity, and solve for the modulation, i.e., the noise-equivalent modulation (NEM). The modulation required by the eye is then determined by multiplying the NEM by the appropriate required S/N factor k.

The input image to be considered is a sine-wave pattern on zero background. Results of measurements made on square-wave test patterns and analysis based on sine-wave functions are easily related (Ref. 14) by the simple Fourier series expansion of the periodic square-wave function. It has been demonstrated (Refs. 6 and 12) that the signal and shot noises of an image formed by scintillations are equal to the difference in the number of scintillations in adjacent image elements and the root-mean-square value of the fluctuations in the difference, respectively. To a good approximation, they are independent of the distribution of scintillations within the image elements. Thus, if one considers a sine-wave modulation pattern on the display, it is necessary to calculate the number of scintillations in [illegible] image elements considered somewhat arbitrarily to be the positive [illegible] tive half cycles of the sine-wave modulation. The [illegible] photoelectron flux density $n_s(x_s)$ generated at the [illegible] is given by

$$n_s(x_s) = \bar{n}_s + \hat{n}_s \sin 2\pi\nu_{os}x_s \tag{44}$$

or

$$n_s(x_s) = \bar{n}_s(1 + M_s \sin 2\pi\nu_{os}x_s) \tag{45}$$

where $\bar{n}_s$ is the average value of the flux density over a period of the test pattern in particles/mm$^2$-sec, $\hat{n}_s$ is the amplitude of the sine-wave modulation, $\nu_{os}$ is the modulation frequency in cycles/mm, and $M_s$ is the modulation amplitude at the photocathode defined by $M_s = (n_s^+ - n_s^-)/(n_s^+ + n_s^-) = \hat{n}_s/\bar{n}_s$, where $n_s^+$ and $n_s^-$ are the peak and valley values of the photoelectron flux density.

If the dynamic response of the PEI system to the modulation is linear and the spatial frequency response of the optical system is uniform over a sufficiently large portion of the field of view, then the luminance of the pattern image on the display is given by

$$n_D(x_D) = \bar{n}_D(1 + M_D \sin 2\pi\nu_{oD}x_D) \tag{46}$$

where, if m is the magnification, $x_D = mx_s$ and $\nu_{oD} = \nu_{os}/m$. The modulation $M_D$ on the display and the modulation $M_s$ at the photocathode are related by $M_D = T(\nu_{oD})M_s$, where $T(\nu_{oD})$ is the frequency response or modulation transfer function discussed in Section IV-E.

If one integrates Eq. 46 over a positive and a negative half cycle of the modulation, takes the difference, assumes that the eye samples one period of the test pattern (Ref. 12), and lets t equal the sampling time, the output signal is given by

$$(N_D^+ - N_D^-)t = (4/\pi)L_D W_D t\bar{n}_D M_D \tag{47}$$

where $N_D^+$ and $N_D^-$ are the respective numbers of photons emitted per second from a positive and negative half cycle of the modulation, $L_D$ is the effective length of the pattern, and $W_D$ is the width of a half period equal to $1/2\nu_{oD}$.

The mean square value of the fluctuations in the difference obtained by adding the mean square values of the fluctuations in each of the half cycles is determined by the scintillation generation rate. Thus, the mean square value of the fluctuations in a sampling period $2W_D$ and a sampling time t is given by

$$G^2 < [(N_D^+ - N_D^-)t/G]^2 > = 2GL_D W_D \bar{n}_D t \tag{48}$$

where G is the mean value of the particle gain, i.e., the number of photons emitted per scintillation. If the noise is measured by the root-mean-square value of the fluctuations, the signal-to-noise ratio at the display is given by

$$(S/N)_D = (2/\pi)M_D(2L_D W_D t\bar{n}_D/G)^{\frac{1}{2}} \tag{49}$$

This expression is simplified by noting that $\bar{n}_D/G$, the scintillation rate on the display, is equal to $\bar{n}_s/m^2$ and $L_D W_D = \epsilon W_D^2 = \epsilon m^2/4\nu_{os}^2$ where $\epsilon$ is the effective length-to-width ratio. Thus, the signal-to-noise ratio on the display is given by

$$(S/N)_D = (2\epsilon\bar{n}_s t)^{\frac{1}{2}} M_D/\pi\nu_{os} \tag{50}$$

Only if the value of $\epsilon$ is sufficiently large can one treat the test pattern in one dimension. It has been stated by Schade (Ref. 7) that the sampling aperture of the eye for lines or bands is the image of the band with the effective length equal to 14 equivalent widths. Therefore, $\epsilon$ should be somewhat greater than 14 so that the luminance of the output image of the pattern will be uniform over a length equal to the sampling aperture of the eye.

Instead of modulation amplitude, it has become customary (Ref. 12) in the analysis of low-light-level television systems to describe the input test pattern by its contrast, as defined by

$$C_s = (n_s^+ - n_s^-)/n_s^+ \tag{51}$$

at the primary photocathode. In Eq. 51, $n_s^+$ and $n_s^-$ are the maximum and minimum values of the primary photoelectron flux density, respectively. The relation between modulation amplitude, defined following Eq. 45, and contrast, defined by Eq. 51, is given by

$$M_s = C_s/(2 - C_s) \tag{52}$$

In terms of the parameters contained in the detailed discussions of low-light-level television systems in Part V of Ref. 8 (e.g., Eq. V-C-18), Eq. 50 for $(S/N)_D$ is given by

$$(S/N)_D/\epsilon^{\frac{1}{2}} = (2/\pi)T(\nu_{os})C_s[0.75t(i_{s\ max}/e)/(2 - C_s)]^{\frac{1}{2}}/N \tag{53}$$

where $i_{s\ max}$, defined by $i_{s\ max} = en_s^+A_T$, and $\bar{n}_s$ are related by

$$\bar{n}_s = (2 - C_s)i_{s\ max}/2eA_T \tag{54}$$

and N, the number of television lines per raster height H, is given by $N = 2H\nu_{os}$. In Eq. 54, $A_T$ is the area of the camera tube target, which is given by $A_T = (4/3)H^2$, if a width-to-height ratio of 4/3 is assumed. Often, the factor $\epsilon^{\frac{1}{2}}$ appearing in Eq. 53 is included implicitly in the $(S/N)_D$. In addition, a factor of $2/\pi$ occurs in Eq. 53 due to the ratio of average signal (used in Eq. 53) to peak signal (used in Part V of Ref. 8).

The average photoelectron flux density is given by

$$\bar{n}_s = \int_0^\infty \eta(\lambda)\bar{n}_{H\lambda}d\lambda \tag{55}$$

where $\eta(\lambda)$ is the quantum efficiency of the photocathode at wavelength $\lambda$ and $\bar{n}_{H\lambda}$ is the average input spectral photon flux density over a sampling period. It is convenient to define

$$\eta = \int_0^\infty \eta(\lambda)\bar{n}_{H\lambda}d\lambda \Big/ \int_0^\infty \bar{n}_{H\lambda}d\lambda \tag{56}$$

and let $\bar{n}_H = \int_0^\infty \bar{n}_{H\lambda}d\lambda$. Then Eq. 55 becomes

$$\bar{n}_s = \bar{\eta}\,\bar{n}_H. \tag{57}$$

In general, it is necessary to perform a numerical integration over the spectral bandwidth of the input image irradiance to determine values of $\bar{n}_s$. However, if the source of irradiance is a standard 2854°K tungsten lamp, then we have $n_s = \sigma_T\bar{H}_T/e$, where $\sigma_T$ and $\bar{H}_T$, discussed in Section IV-B, are the responsitivity and average photocathode irradiance in ma/watt and watt/$m^2$, respectively. In terms of the optical parameters of the objective, the average photoelectron flux density is given by

$$\bar{n}_s = A_o\bar{\eta}\bar{L}/f_o^2 \tag{58}$$

where $A_o$ is the area of the entrance pupil, $f_o$ is the focal length of the objective, and $\bar{L}$ is the average radiance of the sine-wave test pattern in photons/$cm^2$-sec-sterad.

The explicit dependence of the output-image signal-to-noise ratio on the basic parameters of a PEI system can now be given as

$$(S/N)_D = (2etA_o\bar{\eta}\bar{L})^{\frac{1}{2}}T(\nu_{o\alpha})M_s/\pi\nu_{o\alpha} \tag{59}$$

where

- $e$ is the length-to-width ratio of a half period of the test pattern,
- $t$ is the effective integration time of the eye,

$A_o$ is the area of the entrance pupil of the objective,

$\bar{\eta}$ is the mean quantum efficiency defined by Eq. 56,

$\bar{L}$ is the average radiance of the test pattern,

$T(\nu_{o\alpha})$ is the frequency response of the PEI system,

$\nu_{o\alpha} = \nu_{os}/f_o$ is the angular frequency of the test pattern at the entrance pupil in units of cycle/radian, and

$M_s$ is the modulation amplitude of the test pattern.

For a given sampling time and sine-wave test pattern, the output signal-to-noise ratio is proportional to the square root of both the area of the objective and the quantum efficiency of the photocathode and is also proportional to the frequency response.

If we refer to Eq. 50, we see that at a given input irradiance ($\bar{n}_s$ constant), as the frequency of the test pattern increases, the output modulation required for a specified output signal-to-noise ratio increases. It has been determined that if the $(S/N)_D$* is approximately 3.8 (Ref. 15), then the modulation prescribed by Eq. 50 (i.e., 3.8 times the noise-equivalent modulation) approximates the modulation $M_t$ required by the eye for 50 percent detection probability of the image of a test pattern formed by scintillations with unlimited sampling time. Thus, the modulation required by the eye in the presence of shot noise (Ref. 16) is given approximately by

$$M_t = 3.8\pi\nu_{os}/(2\epsilon\bar{n}_s t)^{\frac{1}{2}} \tag{60a}$$

Higher values of $M_t$ would be required if higher detection probability, shorter detection time, or detection under more difficult conditions than that presented by a simple sine-wave pattern were required.

*Often the length-to-width ratio $\epsilon$ of one-dimensional test patterns is included implicitly in the $(S/N)_D$, which then equals approximately 1.1 instead of 3.8.

As the test pattern frequency $\nu_{on}$ approaches zero, $M_t$ does not approach zero as indicated by Eq. 60a. This difficulty with Eq. 60a arises from the limitation imposed by finite viewfield, which prevents maintaining a sufficient value of $\epsilon$ to treat the test pattern as one dimensional. The difficulty appears at roughly 2 cycles/mm on a display viewed through a 7-power eyepiece or 2 cycles/in. on a television display viewed from 50 in.

For low-light-level television systems, it is convenient to express the modulation required by the eye in the form

$$M_t = 3.0\pi N/[6\epsilon(i_s/e)t]^{\frac{1}{2}} \qquad (60b)$$

where N is the number of television lines per raster height, $\epsilon$ is the length-to-width ratio of a half period of the test pattern, t is 0.2 sec, the integration time of the eye, e is the magnitude of the electron charge in coulombs, $i_s = e\,\bar{n}_s(4/3)H^2$ is the total primary photocathode current, and H is the height of a raster on the photocathode. Equation 60b applies to low-light-level television systems with sufficient intensifier gain that the output signal-to-noise ratio is negligibly affected by the video preamplifier noise.

The overall performance of a low-light-level PEI-human eye system at a given scene radiance is essentially specified by the frequency response (modulation transfer) function and the required modulation function of the eye. For example, output modulation functions for several values of input modulation, calculated curves of required modulation for several values of primary photocathode current, and minimum required modulation functions (introduced in Section IV-E) at display luminances of 0.52 cd/m$^2$ and 7.72 cd/m$^2$ are shown in Fig. 13 for a typical triple image intensifier and in Fig. 14 for a typical low-light-level television system. A detailed discussion of the minimum required modulation and the transfer of information from the display to the output of the eye is contained in Appendix A.

Figures 13 and 14 depict the following information:

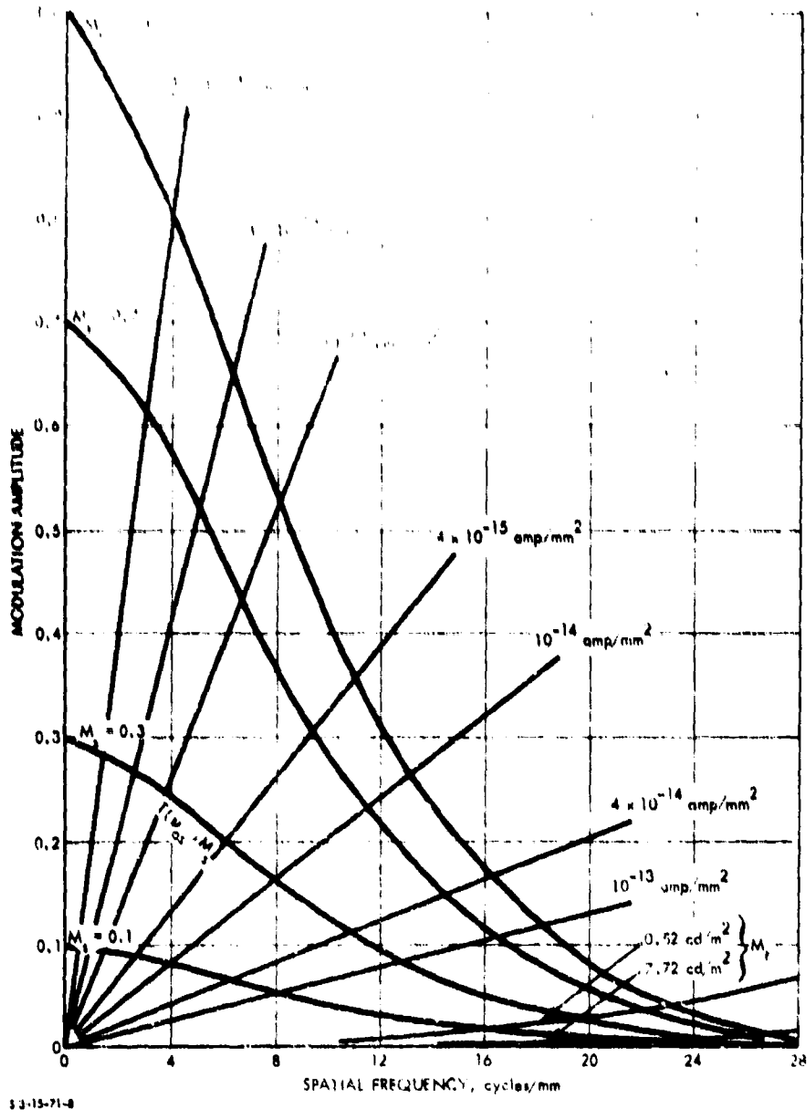


FIGURE 13. (a) Output Modulation of Typical Triple Image Intensifier for Input Modulation Values $M_s$ of 1.0, 0.7, 0.3, and 0.1 and (b) Theoretical Modulation $M_t$ Required by the Eye for Values of Photocathode Current Density $\bar{J}$ of $10^{-16}$, $4 \times 10^{-16}$, $10^{-15}$, $4 \times 10^{-15}$, $10^{-14}$, $4 \times 10^{-14}$, and $10^{-13}$ amp/mm$^2$. Experimental Limiting Required Modulation Curves, Labeled 0.52 cd/m$^2$ and 7.72 cd/m$^2$, are for an M = 7 Ocular.

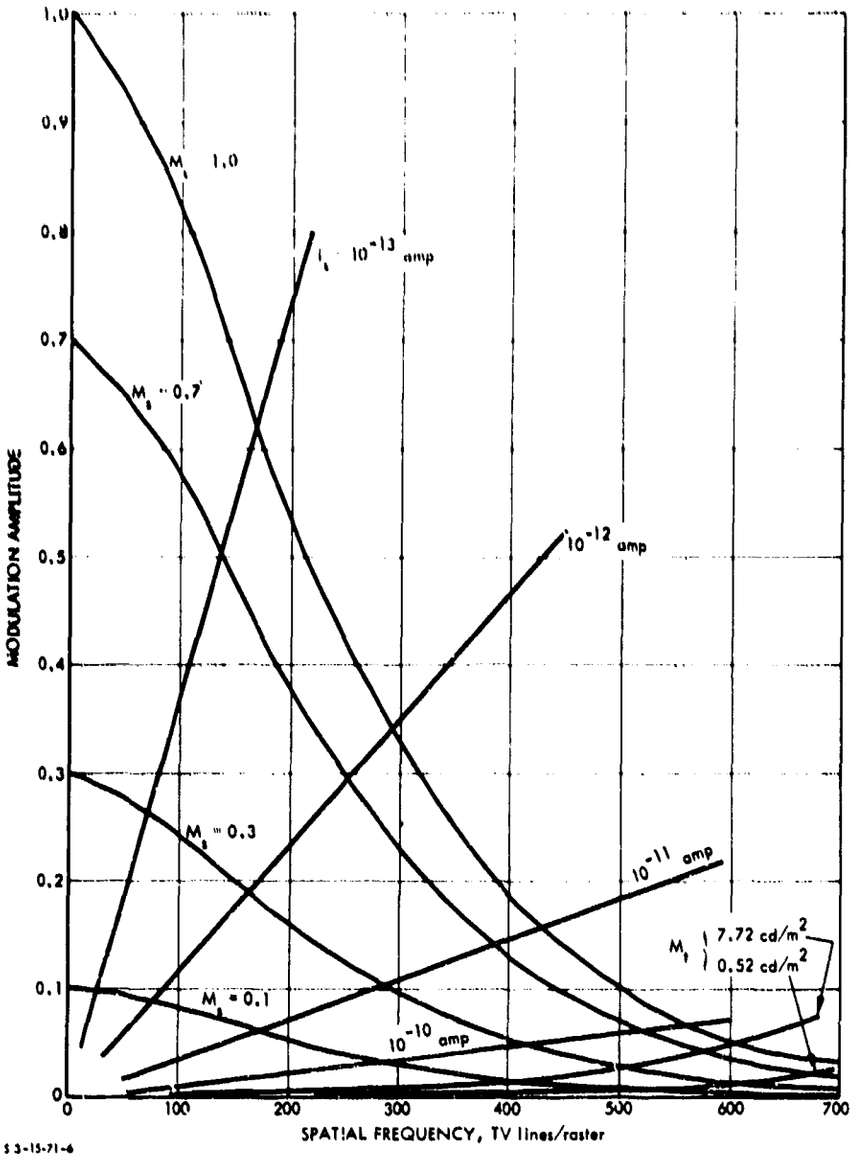


FIGURE 14. (a) Output Modulation of Typical Low-Light-Level Television for Input Modulation Values $M_s$ of 1.0, 0.7, 0.3, and 0.1 and (b) Theoretical Modulation Required by the Eye for Primary Photocathode Current $i_s$ of $10^{-13}$, $10^{-12}$, $10^{-11}$, and $10^{-10}$ amp. Experimental Limiting Required Modulation Curves, Labeled 0.52 cd/m$^2$ and 7.72 cd/m$^2$, are for a Viewing Distance Equal to Three Times the Raster Height.

- The ratio of the output modulation to the required modulation at a given spatial frequency is by Eq. B-1b equal to 1/3.8 times the output signal-to-noise ratio.
- At the intersection of a given output modulation and required modulation curve, the value of the output signal-to-noise ratio is just 3.8, the minimum required for 50 percent detection probability. Hence, for test patterns of a given modulation and radiance, the corresponding value of spatial frequency at the point of intersection is the resolution frequency of the PEI-human eye system, and the range of frequencies from essentially zero to the resolution frequency is the useful bandwidth of the system.

The definition of resolution has been much abused by authors of papers describing the performance of visual systems. Hence, it is important to emphasize that here resolution frequency is defined by the point of intersection of an output modulation and a required modulation curve and thus defines the upper limit of the useful spatial bandwidth of the system. It is also important to note that the resolution frequency and useful bandwidth of low-light-level PEI systems depend not only on the MTF but also on all the system parameters that affect the $(S/N)_D$, as well as the modulation amplitude and the mean radiance of the scene. Furthermore, it is interesting to note that the value of required modulation at the resolution frequency is not 3 percent, as commonly supposed, but depends on the primary photocathode current density determined by the "apparent" radiance of the test pattern, the f-number of the objective, and the mean responsivity of the photocathode. Moreover, the resolution frequency at low input irradiance is not proportional to the square root of the primary photocathode current density but rather is relatively insensitive to it.

The common assumption that resolution frequency is proportional to the square root of the mean responsivity owes its origin to the earliest papers (Refs. 6, 12) on the signal-to-noise theory of resolution, in which the authors did not include consideration of the frequency-response function. This, in effect, amounts to assuming an ideal flat

frequency-response function. For example, in Fig. 13 this assumption would result in the output modulation curves becoming horizontal lines. The intersections of the required modulation curves with these horizontal lines of output modulation would then yield the proportionality of resolution frequency on the square root of mean responsivity. However, due to the rapid roll-off of frequency response with increasing frequency, the resolution frequency is quite insensitive to responsivity. The relationship between graphical representations of the performance of PEI systems by the MTF and required modulation functions on the one hand and the $(S/N)_D$ and resolution functions on the other is discussed in Appendix B.

## B. IMPROVEMENT OF PEI PERFORMANCE

The performance of image-intensifier and low-light-level television tubes is chiefly determined by three parameters:

1. The modulation transfer function (MTF).
2. The effective responsivity of the primary photocathode.
3. The noise introduced by the intensification process.

It is clearly evident that both the MTF and the cathode responsivity of PEI systems should be and can be improved. However, as shown in Figs. 13 and 14, the improvement of cathodes by relatively large factors, which in principle would result in relatively large improvements in resolution at low light levels if the MTF were unity over the frequency range of interest, results in practice in relatively small improvements at the light levels where PEI systems are useful. On the other hand, improvements in MTF will show a direct improvement in PEI resolution and, as shown below, even provide an enhancement of the effect of improvements in cathode responsivity on resolution.

The exploitation of electrooptical technology, principally by the Night Vision Laboratories of the U. S. Army Electronics Command, culminated in the development of the "first generation" of image-intensifier systems. In the design of the first generation, it was

necessary to couple three intensifier stages in cascade to achieve sufficient intensification of low-light-level scenes to view the display without dark adaptation of the eye. But, as shown in Fig. 9, the MTF of image-intensifier and low-light-level television tubes is degraded in proportion to the number of stages which are cascaded to achieve sufficient intensification. Thus, the MTF could be greatly improved if sufficient intensification could be achieved in a single stage without having the intensifier structure degrade the MTF.

To diminish the degradation of MTF occurring in the three-stage, cascade, image-intensifier tubes, a "second generation" of image-intensifier systems was envisioned which would employ a single-stage intensifier tube incorporating a high-gain microchannel plate (MCP). Besides achieving a greatly improved MTF and a reduction in size, it was further believed that the method of fabrication of the MCPs would lead to high production volumes and lower cost.

The MCP image-intensifier tube consists of a fiber-optic faceplate, on the back side of which is formed a photocathode, an electrostatic image-inverting electron lens, an MCP secondary-electron multiplier, and a second fiber-optic plate, on the front side of which is formed a phosphor screen with the usual aluminum film required to prevent light feedback to the photocathode. Image transfer from the MCP to the phosphor depends on the close proximity of these two elements. The electron image generated at the photocathode is focused on the MCP by means of an electrostatic lens. These MCP image-intensifier tubes are customarily called inverter tubes. It is necessary to employ a decelerating electric field to correct the flat image plane presented by the front surface of the MCP. Besides the inverter tubes employing electrostatic focusing between the photocathode and the MCP, considerable effort has been expended in the development of proximity focusing in what is customarily called a wafer tube. Development of the wafer tube has been even less successful than development of the inverter tube.

Unfortunately, of the three objectives of the MCP image-intensifier tube development, only a reduction in size has been achieved. The

expected improvement in MTF has not been achieved. Further, reliability and cost remain problems.

Recent research results (Ref. 17) on silicon transmission secondary-electron multiplication indicate for the first time that sufficient gain can be achieved in a single stage with little degradation of the MTF.

The silicon transmission secondary-electron multiplication (TSEM) dynode consists of a thin (approximately 5 microns--sufficient thickness to be self-supporting) wafer of low-resistivity, P-type silicon, having one surface carefully cleaned and treated with cesium and oxygen to reduce the potential difference between the bulk and vacuum (the effective bulk electron affinity) to zero or less. The dynode is mounted in a vacuum-tube image intensifier with the untreated surface facing the photocathode and the cesium oxide-treated surface facing the phosphor. Photoelectrons generated by the radiant image of the scene focused on the photocathode are accelerated and focused to strike the silicon TSEM dynode with the energy of several thousand electron volts. As the primary electrons penetrate the silicon to a depth of a few thousand angstroms, energy is primarily lost via electron-hole pair production at the rate of approximately 3.6 ev per pair. Some of the resulting excess holes recombine with electrons supplied to an ohmic contact at the periphery of the silicon wafer, while an equal number of excess electrons rapidly thermalize to the temperature of the wafer, diffuse toward the silicon-cesium oxide interface, and escape into the vacuum to maintain current continuity. In a first effort (Ref. 17), 750 secondary electrons per primary electron have been measured at 20 kv, and 230 at 10 kv. Slightly heavier acceptor concentration at the front surface to reduce surface recombination will increase the yield. Photoemission measurements reported earlier (Ref. 18) indicate that the escape probability of excited electrons from cesium- and oxygen-treated, P-type silicon surfaces can be 20 percent or higher. Recent unpublished measurements indicate that an escape probability as high as 50 percent is attainable.

A transmission secondary-emission ratio of at least 500 at 10 kv can be expected. This TSEM gain of 500, multiplied by a diode gain of 50 due to the photocathode-phosphor combination, yields an overall gain of 25,000. An overall gain of 25,000 is ample to view scenes of low radiance down to the limit determined by the photoelectron shot noise without dark adaptation.

The silicon TSEM dynode offers the following advantages over the glass MCP dynode:

- Silicon, unlike glass (a notoriously "dirty" material), is a single element, completely stable chemically, susceptible to ultrahigh purification via zone refining, and susceptible to high-temperature bakeout during tube fabrication to remove any and essentially all adsorbed gases that could damage the photocathode during tube operation. The compatibility of silicon with photocathodes of the S-20 type has been amply demonstrated in the camera tube employing the silicon-diode-array, charge-storage target.
- The solid structure of the TSEM dynode, in contrast to the porous MCP structure, greatly facilitates surface cleansing and removal of adsorbed gases during bakeout, and it reduces the surface-to-volume ratio of the dynode.
- Gain in a silicon TSEM dynode is essentially noiseless. In general, the mean square fluctuation in the number of secondary electrons per incident photoelectron observed for a large number of incident photoelectrons is given by the product of the Fano factor and the mean number of secondary electrons per incident photoelectron. If the distribution of yields is Gaussian or Poissonian, the Fano factor is unity. For the MCP dynode, the Fano factor is generally acknowledged to be greater than unity--approximately 2. For secondary-electron multiplication in semiconductors, the Fano factor is known to be in the range of 0.1 to 0.2.

- The silicon TSEM dynode does not require deposition of an electrode over a portion of the front surface of the dynode. Hence, the collection efficiency for incident photoelectrons is essentially 100 percent, compared to 70 to 80 percent for the MCP dynode. For a 70 percent collection efficiency, the effective responsivity of a 4-ma/watt photocathode is reduced to 2.8 ma/watt.

- Degradation of image-tube MTF by the silicon TSEM dynode ought to be nil compared to the degradation produced by an MCP dynode. The causes of MTF degradation in MCP intensifiers are the broad spread in secondary-electron exit trajectories from adjacent microchannels and the finite size of the microchannels making up the MCP structure. The effect of the broad spread in secondary-electron trajectories is to produce poor proximity focusing in the space between the MCP and the phosphor screen. The origin of the broad spread in secondary-electron trajectories is the high secondary-electron energies coupled with the required accelerating voltage for good phosphor conversion efficiency and limited breakdown field observed in any electron vacuum tube. Typical values of the energy of electrons emerging from an MCP are in the range 10 to 100 ev. On the other hand, in a silicon TSEM dynode, the transmission secondary electrons emerge via thermal diffusion to and across the cesium oxide-vacuum interface with thermal energy equal to only 1/40 ev at room temperature. While some improvement in the MTF of MCP tubes has been achieved via "end spoiling" the channels to restrict the angles of the exiting electrons, the MTF remains comparable to that of a three-stage, first-generation intensifier, despite earlier predictions of a better MTF than even that of a single-stage inverter tube.

It is clear that the microchannel approach is only one of two competing technologies for second-generation image-intensifier tubes, and that the silicon TSEM offers a much greater potential for improvement of MTF and resolution.

To obtain good operation of PEI systems at less than "quarter" moonlight, a continuing effort to improve photocathode responsivity has been pursued. Better methods of manufacturing first-generation image-intensifier tubes have resulted in the improvement of the responsivity of S-20 type photocathodes from 3.5 ma/watt to 5-6 ma/watt, and even 8-9 ma/watt is available, although at lower manufacturing yield and consequently higher cost. Further improvement in photocathode responsivity will depend on the outcome of the long-range effort to develop the cesium oxide-activated, gallium arsenide-type photocathodes and the "third-generation" image tube configurations required to employ them. But, as shown in Figs. 13 and 14, large factors of improvement in responsivity are required to have a significant effect on resolution.

A comparison of the relative improvement in resolution that could be realized with the successful development of the silicon TSEM tube and the improvement realized with a factor-of-two improvement in photocathode responsivity is shown in Fig. 15.

The lower curve in Fig. 15 is the modulation on the screen produced by a three-stage, first-generation image-intensifier tube for a sine-wave test pattern of 30 percent modulation as a function of test pattern frequency. To estimate the relative importance of MTF and responsivity on resolution, consider the line representing the modulation required to provide an S/N ratio of 1.1 as required by the eye for perception of the image of the pattern on the screen of an image intensifier with an S-25 (4 ma/watt) photocathode and irradiance of the test pattern by 0.3 moonlight. All of the modulation-required-by-the-eye versus number-of-lines-per-millimeter curves were calculated on the assumptions that the average reflectivity of the pattern is 20 percent, the objective is effectively f/2, and the S/N ratio required by the eye for this one-dimensional variation in luminance is approximately 1.1. The intersection of the required modulation line for an S-25 cathode and 0.3 moonlight with the three-stage modulation on the screen curve at Point A indicates that the resolution is approximately 12 cycles/mm (line pairs/mm). With this point of intersection as a reference, consider two alternatives for increasing resolution:

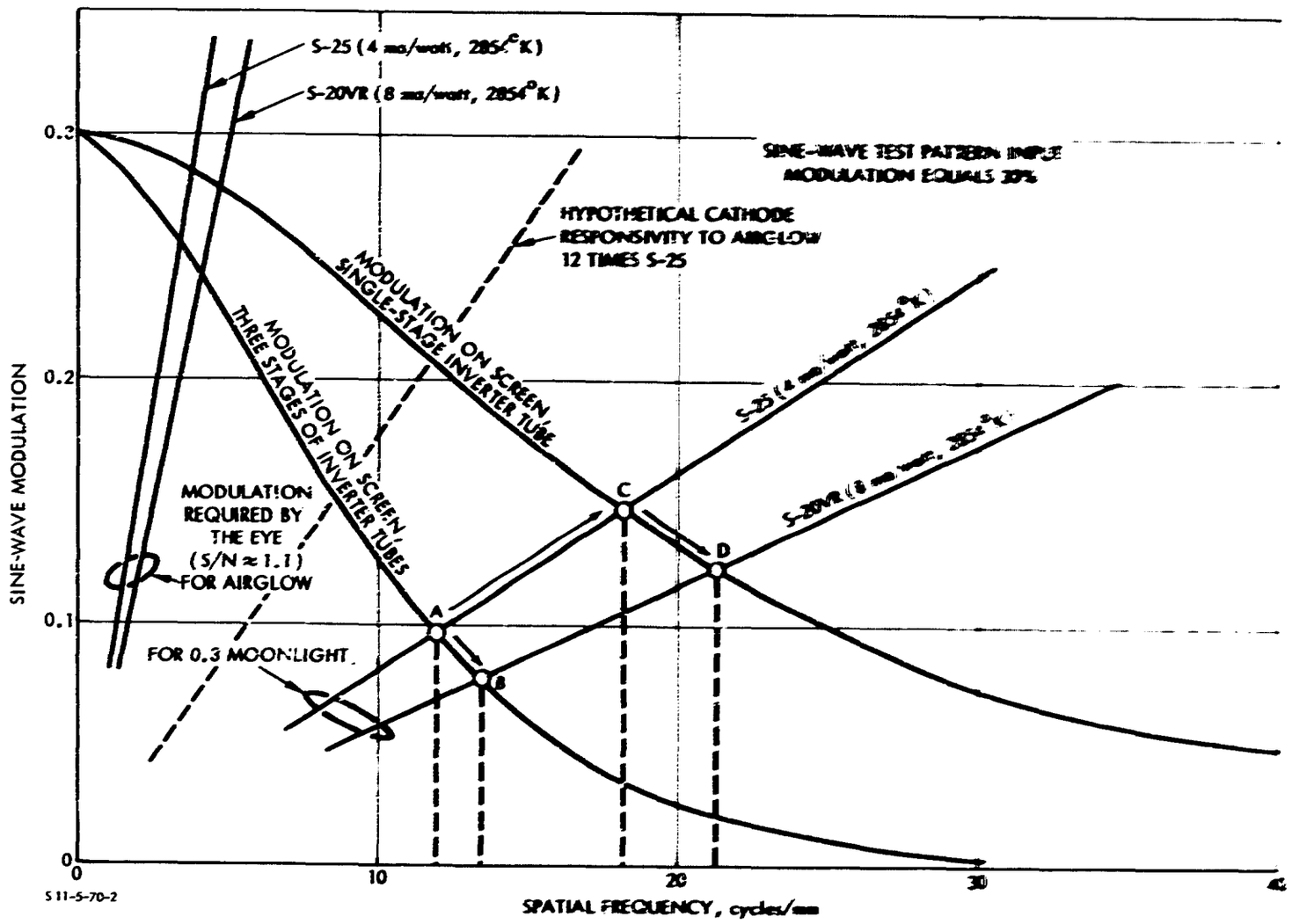


FIGURE 15. Predicted Effect of Cathode Responsivity Versus MTF on Image-Intensifier Performance

1. Choose an S-20VR photocathode with double the responsivity (measured with a standard 2854°K tungsten lamp).

2. Develop a gain structure, the silicon TSEM, which will allow reduction of the number of intensifier stages from three to one with the consequence that the MTF is increased as shown by the two curves of modulation on the screen in Fig. 15.

In the case of higher photocathode responsivity, the resolution would increase from 12 to 13.4 cycles/mm, as indicated by the arrow from A to B. In the case of better MTF, the resolution would increase from 12 to 18.2 cycles/mm, as indicated by the arrow from A to C. It is clear in this example that of the two alternatives for increasing resolution, increasing the MTF is the most effective. Furthermore, by comparison of the arrows from C to D and from A to B, respectively, it is evident that increases in MTF enhance the effect of subsequent increases in cathode responsivity on resolution.

Figure 15 also shows the effects on resolution of changes in responsivity and MTF at the low value of scene irradiance provided by airglow alone (clear night sky, no moonlight). As the irradiance decreases from 0.3 moonlight to airglow, the resolution of a three-stage image intensifier with an S-25 photocathode decreases to such a low value (3 cycles/mm or 75 cycles per diameter with the 25-mm tube used in the starlight telescope) that little improvement can be realized by improving the MTF alone. It is generally acknowledged that with the presently available S-25 photocathodes "quarter" moonlight is required for satisfactory operational performance. Theoretically, the present quarter moonlight performance could be achieved at airglow by increasing the photocathode responsivity to airglow by a factor of approximately 50. Such a large increase in responsivity is <u>not</u> in the offing. However, the dashed line in Fig. 15, respresenting the required modulation with a hypothetical photocathode 12 times more responsive to airglow than the S-25, indicates that by improving the MTF the required improvement in responsivity could be relaxed. An improvement in the MTF to that of a single-stage tube would reduce the required increase in photo-

cathode responsivity from 50 to approximately 12. Thus, it seems clear that the required resolution and operational performance currently realized at quarter moonlight could be achieved with airglow alone in the foreseeable future only if both the responsivity and the MTF were greatly improved.

## VI. CONCLUSIONS

At the present time, greater improvements in the performance of image-intensifier systems can be achieved by improvements in the modulation transfer function than by likely improvements in photocathode responsivity. Therefore, a major effort should be devoted to improving the MTF of image-intensifier tubes by developing the silicon transmission secondary-electron multiplication tube, incorporating existing manufacturable photocathodes, as an alternative to the microchannel plate image-intensifier tube.

A sustained effort of lesser priority to improve photocathode responsivity by developing the cesium oxide-activated, gallium arsenide-type photocathodes should continue. But if a new tube configuration is required, it is essential that the MTF is not sacrificed to achieve better responsivity. Good image-intensifier performance will be realized without depending on either moonlight or artificial irradiance only if <u>both</u> MTF and cathode responsivity are substantially increased.



**Preceding page blank**

## REFERENCES


1. Jurgen R. Meyer-Arendt, Appl. Opt., Vol. 7, p. 2081, 1968.

2. Institute for Defense Analyses, Luminance, Radiance, and Temperature, IDA Research Paper P-339, Lucien M. Biberman, August 1967.

3. A.C. Hardy and F.H. Perrin, The Principles of Optics, McGraw-Hill, New York, 1932.

4. C.H. Graham, Vision and Visual Perception, John Wiley and Sons, Inc., New York, 1965.

5. Brown, Graham, Leibowitz, and Ranker, J. Opt. Soc. Am., Vol. 43, p. 197, 1953.

6. A. Rose, J. Opt. Soc. Am., Vol. 38, p. 196, 1948; Advances in Electronics, Vol. 1, p. 131, 1948.

7. Otto H. Schade, J. Opt. Soc. Am., Vol. 46, p. 721, 1956.

8. Institute for Defense Analyses, Low-Light-Level Devices: A Sensor Components Manual for Systems Designers, IDA Report R-169, Lucien M. Biberman, Alvin D. Schnitzler, Frederick A. Rosell, and Harry L. Snyder, in publication.

9. A. van Meeteren, paper presented at Optical Society of America meeting, Chicago, Ill., October 21-24, 1969.

10. W.N. Charman and A. Olin, Photo. Sci. Eng., Vol. 9, p. 385, 1965.

11. Otto H. Schade, RCA Review, Vol. 26, p. 460, 1967.

12. J.W. Coltman, J. Opt. Soc. Am., Vol. 44, p. 1168, 1954.

13. J.W. Coltman and A.E. Anderson, Proc. IRE, Vol. 48, p. 858, 1960.

14. J.W. Coltman, J. Opt. Soc. Am., Vol. 44, p. 468, 1954.

15. Richard Legault in Photoelectronic Imaging Devices, Lucien M. Biberman and Sol Nudelman, eds., Plenum Press, New York, 1971.


**Preceding page blank**

16. Institute for Defense Analyses, Overall Performance of Photoelectronic Imaging Systems, IDA Note N-727(R), Alvin D. Schnitzler, May 1970; Proc. 18th IRIS, to be published.

17. R. U. Martinelli, Appl. Phys. Letters, Vol. 17, p. 313, 1970.

18. R. U. Martinelli, Appl. Phys. Letters, Vol. 16, p. 261, 1970.

## APPENDIX A

### IMAGE INFORMATION TRANSFER, DISPLAY TO EYE

To understand the significance of the minimum required modulation curves introduced in Section IV-E and shown in Figs. 13 and 14, it is necessary to consider the signal-to-noise ratio $(S/N)_E$ at the output of the eye as a function of the particle gain G. (The particle gain is given by $G = m^2\bar{n}_D/\bar{n}_s$, the number of photons emitted by the output display per photoelectron emitted by the primary photocathode.) The calculation of $(S/N)_E$ requires a distinction to be made between two cases defined by $G > 1/\eta_E\eta_c$ and $G < 1/\eta_E\eta_c$, respectively, where $\eta_E$ is the quantum efficiency of the eye and $\eta_c$ is the collection efficiency of the eye or ocular. The collection efficiency of the eye is given by $\eta_c = \rho_E^2/S^2$ and of an ocular by $\eta_c = \rho_E^2\mathfrak{m}^2/254^2$, where $\rho_E$ is the radius of the entrance pupil of the eye in millimeters, S is the separation between a display and the eye, and $\mathfrak{m}$ is the subjective magnification of an ocular.

The quantity $\eta_E\eta_c G$ equals the number of photons detected by the eye per primary photoelectron. In the first case, $\eta_E\eta_c G$ is greater than unity, so that each primary photoelectron initiates a visual response by the eye--the quantum transfer efficiency from the primary photocathode to the output of the eye is unity. Consequently, the signal and shot noise, respectively, at the output of the eye are

$$S_E = \eta_E\eta_c(2/\pi)(2L_D W_D \bar{n}_D t)T_E(\nu_{oD})M_D(\nu_{oD}) \qquad \text{(A-1)}$$

and

$$\sigma_E = \eta_E \eta_c G(2L_D W_D \bar{n}_D t/G)^{\frac{1}{2}} \tag{A-2}$$

and $(S/N)_E$ is given by

$$(S/N)_E = (2/\pi)(2L_D W_D \bar{n}_D t/G)^{\frac{1}{2}}\ T_E(\nu_{oD}) M_D(\nu_{oD}) \tag{A-3}$$

where

$$G > 1/\eta_c \eta_E.$$

In the second case, $\eta_E \eta_c G$ is the fraction of primary photoelectrons which, on the average, initiate a visual response by the eye. Thus, in this case, the quantum transfer efficiency is equal to $\eta_E \eta_c G$. The signal and shot noise, respectively, are given by

$$S_E = \eta_E \eta_c (2/\pi)(2L_D W_D \bar{n}_D t) T_E(\nu_{oD}) M_D(\nu_{oD}) \tag{A-4}$$

and

$$\sigma_E = (\eta_E \eta_c)^{\frac{1}{2}}\ (2L_D W_D \bar{n}_D t)^{\frac{1}{2}} \tag{A-5}$$

The signal-to-noise ratio at the output of the eye is given by

$$(S/N)_E = (\eta_E \eta_c)^{\frac{1}{2}}\ (2/\pi)(2L_D W_D \bar{n}_D t)^{\frac{1}{2}}\ T_E(\nu_{oD}) M_D(\nu_{oD}) \tag{A-6}$$

where

$$0 < G < 1/\eta_c \eta_E.$$

Careful examination of Eq. A-6 reveals that, for a given display luminance $\bar{n}_D$, the signal-to-noise ratio at the output of the eye is independent of G and $\bar{n}_s$. If G increases, the corresponding decrease in $\bar{n}_s$ is compensated by an increase in the quantum transfer efficiency.

However, if $G > 1/\eta_E\eta_c$, consideration of Eq. A-3 reveals that for a given value of $\bar{n}_D$ the $(S/N)_E$ decreases in proportion to $1/G$ or $\bar{n}_s$ as G increases.

In the vicinity of $G = 1/\eta_E\eta_c$, neither Eq. A-3 nor Eq. A-6 is accurate due to the statistical distribution of the particle gain about its average value. As G increases and approaches $1/\eta_E\eta_c$, the particle gain of an increasing number of photoelectrons exceeds $1/\eta_E\eta_c$, causing the $(S/N)_E$ to fall below the value predicted by Eq. A-6. When G increases above $1/\eta_E\eta_c$, the particle gain of a decreasing number of photoelectrons fails to exceed $1/\eta_E\eta_c$, and the $(S/N)_E$ approaches the value determined by Eq. A-3. The relative dependence of the $(S/N)_E$ over the complete range of G is illustrated in Fig. A-1.

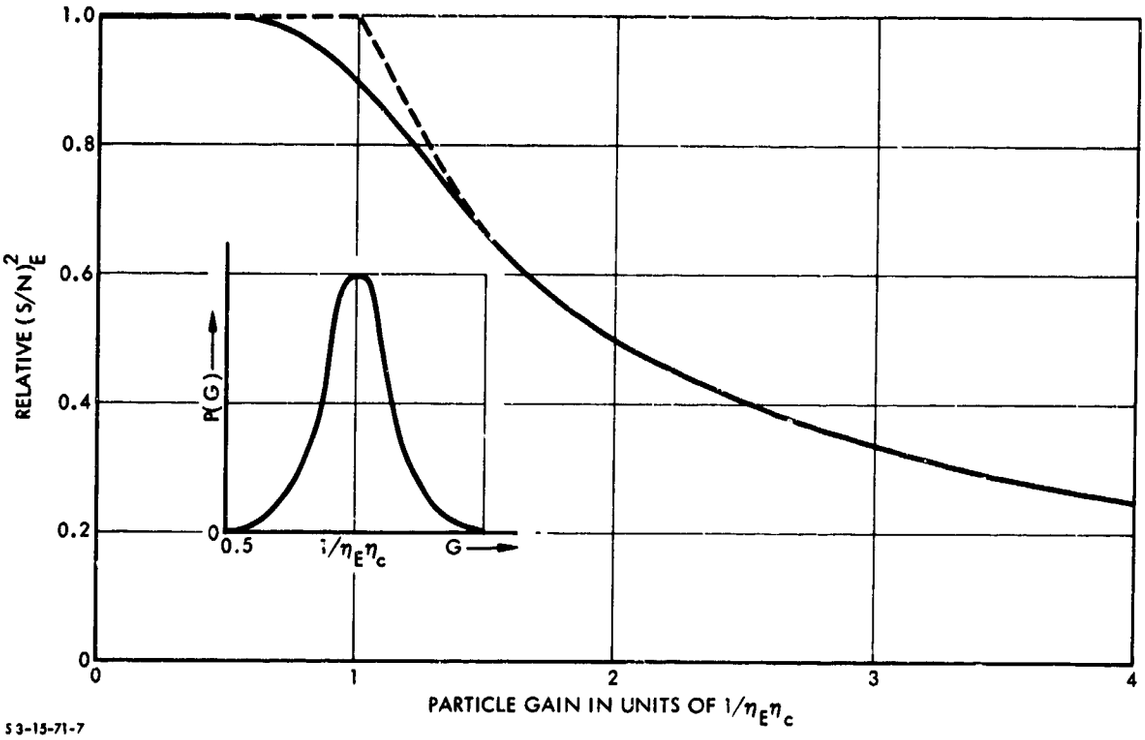


FIGURE A-1. Signal-to-Noise Ratio Squared at the Output of the Eye Versus Particle Gain at a Fixed Display Luminance. Insert Centered at Average Particle Gain Equal to $1/\eta_E\eta_c$ is Probability of Gain P(G) Versus Gain G.

Under normal operating conditions, the particle gain of a low-light-level PEI system exceeds $1/\eta_E\eta_c$, so that the quantum transfer efficiency is unity, as assumed in the derivation of Eq. 49 for the $(S/N)_D$. In image intensifiers, for example,

$$1/\eta_E\eta_c = 254^2/\eta_E\rho_E^2 m^2. \qquad \text{(A-7)}$$

For typical values of the parameters, such as $\eta_E = 0.01$ (Ref. 2) for green light, $\rho_E = 1$ mm and $M = 7$, the value of $1/\eta_E\eta_c$ is approximately $1.3 \times 10^5$. Typical manufacturers' data sheets report that with a standard 2854°K tungsten source and a photocathode responsivity of 4 ma/watt, an input irradiance of $10^{-6}$ watt/ft$^2$ results in an output luminous exitance of 1 lumen/ft$^2$. The resulting particle gain, given by $G = m^2\bar{n}_D/\bar{n}_s$, is equal to $1.6 \times 10^5$, somewhat greater than required for unity quantum transfer efficiency. (The magnification m in the above example is unity.) For a low-light-level television system

$$1/\eta_E\eta_c = S^2/\eta_E\rho_E^2 \qquad \text{(A-8)}$$

and if $S = 30$ in., $\eta_E = 0.01$, and $\rho_E = 1$ mm, $1/\eta_E\eta_c$ is approximately equal to $5.8 \times 10^7$. In practice, typically $m = 10$, and the luminous exitance of the display equals 10 lumen/ft$^2$. Thus, the resulting particle gain is approximately $1.6 \times 10^8$, nearly a factor of three greater than required for unity transfer efficiency.

If the procedure for determining the modulation on the display required by the eye is followed by setting $(S/N)_E$, given by Eq. A-3 or Eq. A-6, equal to 3.8, the minimum required by the brain for 50 percent detection probability, then for a given value of $\bar{n}_D$ and for $G < 1/\eta_E\eta_c$, the required modulation $M_t(\nu_{oD})$ is minimal and independent of G, and for $G > 1/\eta_E\eta_c$ the required modulation increases in proportion to G. The experimental determination of $M_t(\nu_{oD})$ reported by van Meeteren (Ref. 1) was made by illuminating variable transmission transparencies with a tungsten lamp for viewing by the unaided eye. The conditions of the experiments correspond to setting G equal to unity,

which is much less than $1/\eta_E\eta_c$. Hence, the $(S/N)_E$ is given by Eq. A-6, and the required modulation functions at each value of luminance are minimal, as indicated in Figs. 13 and 14.

Further consideration of Eq. A-6 reveals that it could be employed along with van Meeteren's data for $M_t(\nu_{oD})$ to deduce the frequency response function of the eye $T_E(\nu_{oD})$. It should be noted that $T_E(\nu_{oD})$ does not equal $1/M_t(\nu_{oD})$, as is often assumed. It depends on several other factors as well, which appear in Eq. A-6.

It should also be observed that Eq. 49 was derived for low-light-level PEI systems on the assumption, based on experimental evidence, that the signal-to-noise ratio at the display is identical with the signal-to-noise ratio at the output of the eye. However, the results of our derivations, Eqs. 49 and A-3, indicate that they differ by the factor $T_E(\nu_{oD})$. In actual fact, neither equation is strictly correct, for if the noise is represented by its power spectra, it is apparent that higher frequency components are attenuated by the roll-off in the frequency response of both the PEI device and the eye. In practice, the fact that good, experimental agreement is observed with Eq. 49 indicates that the additional attenuation of signal at high frequencies by the roll-off of the frequency response of the eye is compensated by neglect of the high-frequency attenuation of noise by the frequency response of both the PEI device and the eye.

## APPENDIX A REFERENCES


1. A. van Meeteren, paper presented at Optical Society of America meeting, Chicago, Ill., October 21-24, 1969.

2. R. Clark Jones, J. Opt. Soc. Am., Vol. 49, p. 645, 1959.

## APPENDIX B

### REQUIRED MODULATION, SIGNAL-TO-NOISE RATIO, AND RESOLUTION

From Eqs. 50 and 60, the output signal-to-noise ratio for both image-intensifier and low-light-level television systems, in terms of $M_t$, is given by

$$(S/N)_D = 3.8T(\nu_{oD})M_s/M_t \tag{B-1a}$$

or

$$(S/N)_D = 3.8M_D(\nu_{oD})/M_t. \tag{B-1b}$$

Values of $(S/N)_D$ at a set of values of $\nu_{os}$ are usually determined graphically from a measured $M_D(\nu_{oD})$ curve and plot of $M_t(\nu_{oD})$ given by either Eq. 60a or Eq. 60b. For given values of $M_s$ and of $\bar{j}_s$, the $(S/N)_D$, as a function of $\nu_{os}$, can be determined at a sufficient number of points to form a smooth curve. The results of such a determination for $M_s = 1$ and $\bar{j}_s = 10^{-16}$, $10^{-15}$, $10^{-14}$, and $10^{-13}$ amp/mm$^2$, respectively, are shown for the triple image intensifier in Fig. B-1. The intersections of the $(S/N)_D$ curves with the line at $(S/N)_D = 3.8$ define the resolution of the triple image intensifier at each specified average photocathode current density and input test pattern modulation equal to unity. Similar graphs of $(S/N)_D$ versus $\nu_{os}$ are presented in sections of Ref. 1 concerned with specific low-light-level television systems.

By referring again to Eq. 50 and the relation $M_D = T(\nu_{oD})M_s$, it is observed that at a given input modulation ($M_s$ constant), as the

**Preceding page blank**

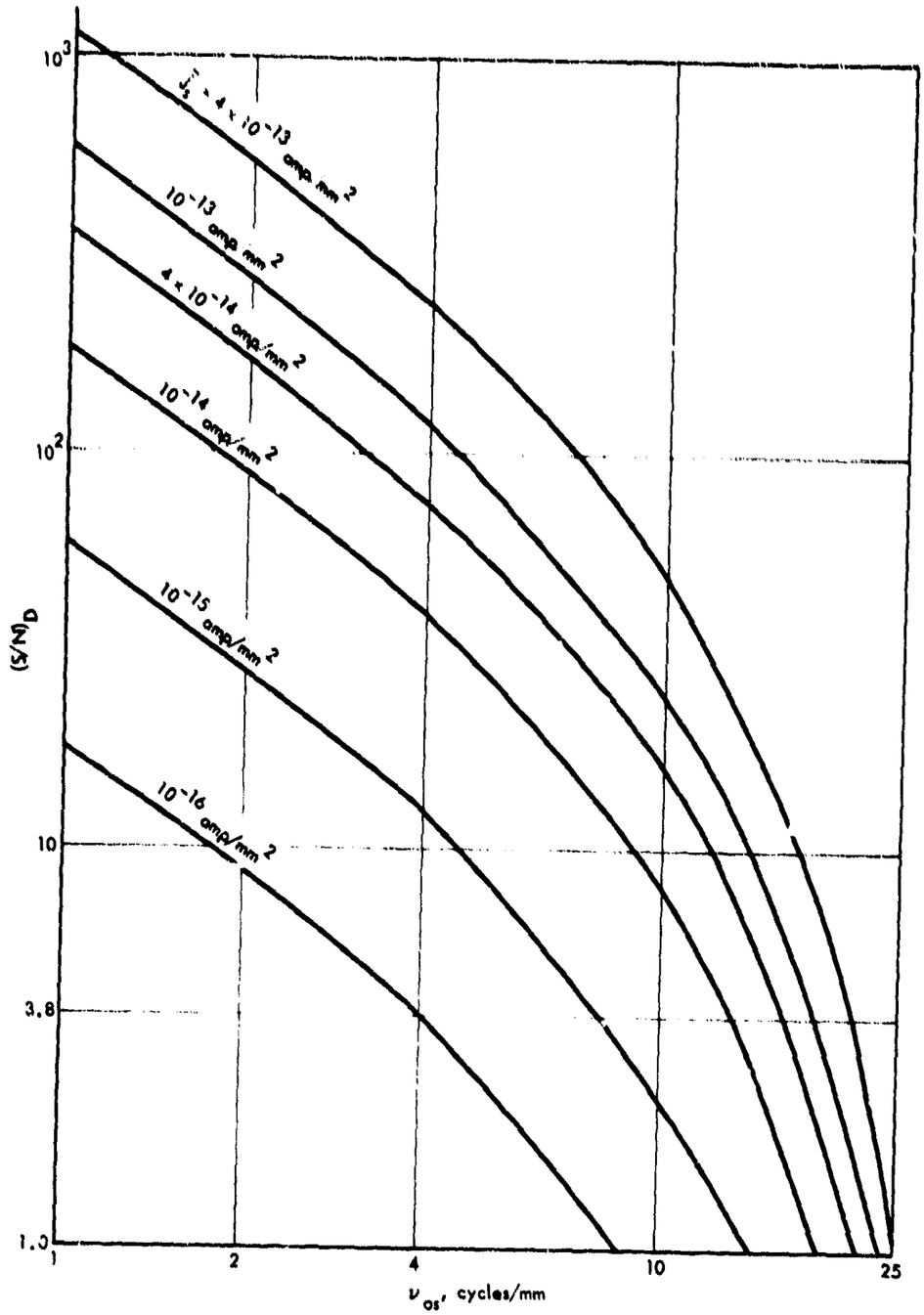


FIGURE B-1. Display Signal-to-Noise Ratio Versus Test Pattern Frequency on Photocathode for Photocathode Current-Density Values $\bar{j}_s$ of $10^{-16}$, $10^{-15}$, $10^{-14}$, $4 \times 10^{-14}$, $10^{-13}$, and $4 \times 10^{-13}$ amp/mm$^2$. (Note Signal-to-Noise Ratio of 3.8 Required for 50% Detection Probability by Observer.)

input irradiance or $\bar{n}_s$ increases, the spatial frequency must be increased to maintain a specified value of $(S/N)_D$. If $(S/N)_D$ is set equal to 3.8, the minimum required by the eye, then Eq. 50 approximates the relation between the subjective resolution of the eye and $\bar{n}_s$ for a given value of $M_s$. The explicit relation between $\nu_{os}$ and $\bar{n}_s$ is not generally available because, as noted above, $T(\nu_{oD})$ is usually known only empirically. However, $\nu_{os}$ as a function of $\bar{n}_s$ for a given value of $M_s$ can be determined graphically from the simultaneous plots of output modulation $M_D(\nu_{oD})$ and required modulation $M_t(\nu_{oD})$ shown in Fig. 13.

The resolution as a function of average photocathode current density determined from Fig. 13 is shown in Fig. B-2 from $M_s$ = 1.0, 0.7, 0.3, and 0.1. As the photocathode current density increases, eventually the resolution saturates. This result occurs because, as the photocathode current density increases, the required modulation approaches the limiting required modulation curves. The intersections of the two limiting required modulation curves shown in Fig. 13 with the $M_D(\nu_{os})$ curves yield the saturation values of the resolution at the specified display luminance. For a given intensifier gain, the display luminance increases with photocathode current density. Thus, the saturation resolution will lie somewhere between the values determined by the $M_t(\nu_{os})$ curves for 0.52 cd/m$^2$ and 7.72 cd/m$^2$.

The resolution as a function of photocathode current density or input-image irradiance is often determined subjectively and plotted in the manner of Fig. B-2. From such experimental data and the measured $M_D(\nu_{os})$ curves for corresponding values of input modulation, subjective curves of required modulation versus spatial frequency at a given value of photocathode current density can be deduced and plotted in the manner of Fig. 13.

Of the graphical forms described above for representing the dependence of overall performance of a PEI system and human observer on signal and noise, that of Fig. 13 seems preferable. An important advantage of Fig. 13 is that, to a good approximation, at least, the dependence of the $(S/N)_D$ on the frequency-response function and the

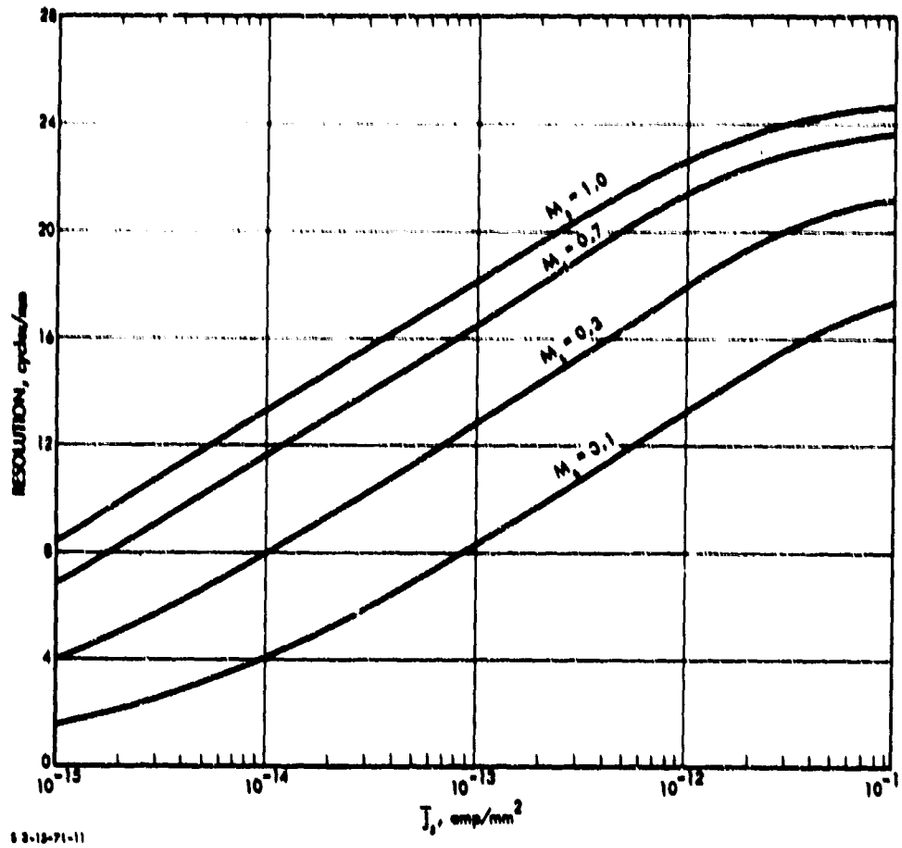


**FIGURE B-2. Resolution Versus Photocathode Current Density for Input Modulation Values of 1.0, 0.7, 0.3, and 0.1**

photocathode current density is shown explicitly. In particular, the effects of photocathode current density and frequency response on resolution (the highest spatial frequency at which the $(S/N)_D$ is equal to or greater than 3.8, the minimum required by the eye) are readily deduced from Fig. 13 by noting the intersections of the required and output modulation curves. For example, if $M_s = 0.3$ and if $J_s$ is increased from $10^{-14}$ to $10^{-13}$ amp/mm$^2$ by increasing either the photocathode irradiance or quantum efficiency by a factor of 10, the resolution would increase from approximately 8 to 13 cycles/mm.

If it is anticipated that a PEI system will be used for detection of images of all sizes on the display, then the overall performance of a PEI system and an observer will depend on the $(S/N)_D$ ratio at all frequencies weighted equally. If the scene comprised a random distribution of image element sizes such that the frequency distribution were white, then the $(S/N)_D$ ratio of the scene would be roughly proportional to the ratio of the area under the output modulation curve to the area under the required modulation curve. This differs somewhat from the overall image quality measure of aerial photography discussed in Part II of Ref. 1. The latter, defined as the area bounded by the output and required modulation curves, is proportional to output signal minus noise. Since detection probability is a monotonically increasing function of $(S/N)_D$ and $(S-N)_D$ increases with $(S/N)_D$, correlation of the detection probability with either the ratio or the difference will yield equally good results. The S/N ratio is preferable from the standpoint of analysis, however, because it is a fundamental parameter of decision and information theory.

In addition to the PEI system and observer, it is useful to specify a measure of the performance of a PEI system without reference to the eye. Such a measure should maximize the S/N ratio of the image on the display. The definition of detection efficiency (Ref. 2) for infrared point detectors can be logically extended (Ref. 3) to imaging systems by utilizing the image S/N ratio. The input image S/N ratio of a sine-wave-modulated incident photon flux is given by

$$(S/N)_H^2 = 2L_s W_s t\bar{n}_H. \qquad \text{(B-2)}$$

If the image detection efficiency D is defined by

$$D = (S/N)_D^2/(S/N)_H^2 \qquad \text{(B-3)}$$

then for a shot-noise-limited PEI system one obtains

$$D_{\nu o} = \bar{\eta}\, T^2(\nu_{os}) \qquad \text{(B-4)}$$

at frequency $\nu_{os}$ on the sensor. The effects of internal noise could be included in the expression for D but do not appear here because one has assumed negligible dark current and sufficient intensifier gain for shot noise to be dominant.

For a scene that comprised a random distribution of image element sizes such that the frequency distribution were white, performance would be proportional to the integral of Eq. B-4 over all frequencies and the image detection efficiency would be given by

$$D = \bar{\eta} \int_0^{\infty} T^2(\nu_{os})\, d\nu_{os}. \qquad \text{(B-5)}$$

This integral will be recognized as the noise-equivalent bandwidth as defined by Schade (Ref. 4). Therefore, the performance of a PEI system by itself, with sufficient intensifier gain to produce a shot-noise-limited image and negligible dark current, is proportional to the product of the quantum efficiency of the sensor and the noise-equivalent bandwidth of the system.

## APPENDIX B REFERENCES


1. Institute for Defense Analyses, Low-Light-Level Devices: A Sensor Components Manual for Systems Designers, IDA Report R-169, Lucien M. Biberman, Alvin D. Schnitzler, Frederick A. Rosell, and Harry L. Snyder, in publication.

2. R. Clark Jones, Proc. IRE, Vol. 47, p. 1495, 1959.

3. Institute for Defense Analyses, Overall Performance of Photoelectronic Imaging Systems, IDA Note N-727(R), Alvin D. Schnitzler, May 1970; Proc. 18th IRIS, to be published.

4. Otto H. Schade, Jour. SMPTE, Vol. 58, p. 181, 1952.